ADDIS ABABA UNIVERSITY

SCHOOL OF GRADUATE STUDIES

INFLUENCE OF CONTROLLED LIGHT INDUCED DEGRADATION ON HYDROGENATED AMORPHOUS SILICON (a-Si:H) SOLAR CELL PARAMETERS

By

YESHITILA G.MICHEAL

MARCH 1994

ADDIS ABABA

INFLUENCE OF CONTROLLED LIGHT INDUCED DEGRADATION ON HYDROGENATED AMORPHOUS SILICON (a-Si:H) SOLAR CELL PARAMETERS

By

YESHITILA G.MICHEAL

A THESIS SUBMITTED TO

THE SCHOOL OF GRADUATE STUDIES

ADDIS ABABA UNIVERSITY

IN PARTIAL FULFILMENT

OF THE REQUIREMENT FOR THE DEGREE OF

MASTER OF SCIENCE IN PHYSICS

MARCH 1994

ADDIS ABABA

ACKNOWLEDGEMENTS

I am extremely grateful to Prof. H.Wagner who has enabled me to join the research group at the Institute of Thin Film and Ion Technology (ISI/PV), KFA-Julich ,Germany.I am also greatly indebted to my advisor Dr.Thomas Eichoff for his constant assistance, invaluable guidance and friendly encouragement without any reservation during the whole period of my research work at the Institute.

I would like to express my due thanks to all members of the group "Solar Cell Characterization" for their Unreserved assistance while I was carrying out my experiments and also for stimulating discussions on the interpretation of data. I am particularly grateful to Mr. F.Birmans and Mr. W.Reetz for their encouragement and continued follow up of the experimental work. Also, many thanks to Dr.C.Beneking who supplied me with samples. My special thanks goes to Mr. B,Rech and Ms. K.Winz whose valuable suggestions useful advises accounted a lot when I faced problems.

It is my pleasure to express my heartfelt gratitude to my advisor and instructor Dr. I. M. Kashirski, Addis Ababa University, for his constructive criticisms and comments.

On behalf of the Alemaya University of Agriculture , I want to extend my appreciation to the Deutscher Akademischer Austauschdients (German Academic Exchange Service) DAAD - for the financial support I received during my stay in Germany, without which the work would not have been possible. My thanks are also due to Dr. F. Dworschak who spent much of his precious time looking for a qualified and appropriate advisor in the area I proposed to work the research.

Finally, I would like to extend my deepest thanks and appreciations to my friends Ato Tensay Kumbi and W/t Rebecca Yilma who have helped me in typing part of my thesis paper. I am also thankful to Ato Meseret Abeje who read part of the manuscript and Ato Tufa Dinku who assisted me in editing the thesis. Also, I am greatly thankful to Ato Daniel Hailu for his continued encouragement to complete this work.

CONTENTS

Chapter 4. Influence of Controlled Light- Induced Degradation on a-Si:H Solar Cell Parameters

Abstract

*The influence of controlled light induced degradation on hydrogenated amorphous silicon (a-Si:H) based solar cell parameters was studied using low intensity (AM1.5) and high intensity (~10AM1.5) illuminations obtained from WACOM solar simulator. The light soaking experiments were done on two types of structures, namely, pin and pinpin solar cells. The devices were prepared by plasma enhanced chemical vapour deposition (PECVD) technique in a commercial 3-chamber PECVD systems on 10*10 cm^2 glass substrate. The effect of various factors such as temperature, i-layer thicknesses, etc., on the degradation behavior of a-Si:H solar cells were investigated. The paper presents the experimental results obtained from light soaking tests on pin and pinpin samples under these different conditions.*

Introduction

Until now fire wood and other plant fuels have been the prime sources of energy for people in many developing countries. The combustion of wood and other products, such as charcoal, are being extensively used in these societies for cooking, heating and other purposes such as drying, lighting a house, etc. Due to increased prices of petroleum products, whose supply does not meet the demand , and due to lack of purchasing power, firewood and charcoal will probably remain or even become more important for large number of people in the future. The wide practice of burning wood and charcoal to satisfy the energy demand of fast growing population has a big impact on the environment in that the use of firewood causes deforestation while the use of charcoal affects the environment in connection with deforestation as well as carbonization of the atmosphere.

While deforestation causes an imbalance of climate which in turn leads to protracted droughts as was evident in many developing countries, carbonization of the atmosphere is the main reason for the global warming. Thus, nowadays a lot of efforts are being made in order to find better sources of energy which are friendly to the environment, cost effective, have high reliability and can improve the quality of life in remote areas. Among these solar energy is the main source of energy for many African countries and other developing countries.

Solar energy conversion technology offers unparalleled potential for replacing firewood in many countries which have both good average insolation rates and large number of people in rural and remote areas that are not connected to public power grids. Thus, this technology is an ideal solution in these

countries to satisfy the increasing demand of energy as well as to preserve the environment.

There are a number of systems, such as photovoltaic, solar thermal and photoelectrochemical systems, which use solar radiation to provide energy for our daily life. In the photovoltaic technology direct sunlight is converted into electricity by the use of photovoltaic (PV) cells sometimes called solar cells. This technology has many applications. For instance, PVs are capable of supplying electricity to remote areas, powering water pumping systems for irrigations or other agricultural activities, powering of cooling systems, such as refrigerators which may be needed for preservation of vaccines and other medical equipments in remote health stations, etc.

Various types of solar cells are used to convert sunlight for power use. Single-crystal silicon has been the material of choice for high-performance, highly reliable solar cells since the successful deployment of silicon photovoltaic systems for space power. Most of the terrestrial photovoltaic power systems sold today are crystalline silicon. However, with regard to the cost of manufacturing, crystalline silicon is not the most promising type of solar cell.

Crystalline silicon is made by growing large cylindrical single crystals, called boules. The boules are sliced into thin wafers, from which photovoltaic devices are made. Slicing is an expensive and material-wasteful process. Thus, the need to lower the cost of terrestrial photovoltaic power has focused research efforts on alternative materials as well as on less expensive means of producing solar-grade silicon.

A less expensive material, polycrystalline silicon, by-

passes the expensive and energy-intensive crystal growth process. However, thin films are found to be the most promising type of materials in manufacturing less costly solar cells.

The lowest-cost approach would be to minimize the required amount of semiconductor material. Thin films have been developed that are only a few micrometers thick. Such films are produced by a number of vapour deposition approaches carried out with in-line, highly automated systems. The techniques are adaptable to a number of semiconductor materials that are optimized for solar cell operation. Thin films are cheaper than crystalline structures but typically have lower efficiencies. Ultimately, however, thin films will be necessary for producing low-cost electricity, because the bottom line - the cost per watt - is more important than the efficiency.

In general, since the first practical solar cell at Bell laboratories in 1954, considerable progresses have been achieved in improving the conversion efficiency of different solar cells. The highest-efficiency single-junction solar cells are made from crystalline silicon and GaAs. Silicon cells of 23% efficiency and GaAs cells of 25% efficiency have been confirmed. When the same materials are used in concentrator applications, the efficiencies increase to 28% and 29%, respectively. The highest efficiency that has been confirmed is 34% for a GaAs-GaSb stacked cell operating at 100-Suns concentration - light concentrated to an intensity 100 times that of ordinary sunlight. For 1-Sun conditions, the efficiency of polycrystalline silicon is approximately 18%; that of cells made using the edge-defined film-fed growth-ribbon process, 14%; and that of dendritic web cells, 15.5%[1].

The highest thin film cell efficiency has been confirmed at

15.8%, for cadmium telluride. Thin films of silicon on ceramic substrates have yielded efficiencies of 15.7%; copper indium diselenide, 12-13% (almost 16% has been achieved by the addition of gallium); and amorphous silicon, 12% before light soaking[1].

Amorphous silicon (a-Si) based solar cells are very promising as low cost and large area devices for solar energy conversion, but their application is still limited because of the degradation observed under long sunlight exposure. In the past decades considerable progresses have been achieved in improving the initial conversion efficiency of hydrogenated amorphous silicon (a-Si:H) solar cells. But, improving only the initial efficiency is not sufficient without reducing the loss in efficiency due to sun light exposure. Thus, much emphasis is also given in improving the stability of a-Si:H solar cells.

One of the major steps towards the suppression of degradation in a-Si:H solar cells is a better understanding of light-induced degradation behaviour of the solar cells. The understanding of this behaviour is very essential in that it gives a knowledge how to surmount the problem of a decrease in efficiency under illumination. Moreover, a better understanding of degradation behaviour enables to identify the best working condition for a-Si:H solar cells. For instance, the degradation of a-Si:H solar cells is found to be smaller when light soaking takes place at higher temperature. This feature is very important in that it gives a clue that a-Si based solar cells operate at relatively higher efficiencies when the cells are working in summer or in tropical areas.

We have, therefore, performed a number of low intensity and high intensity light soaking tests to study the influence of controlled light-induced degradation on the performance of

a-Si:H solar cells. The devices were prepared by plasma enhanced chemical vapour deposition(PECVD) technique using a 3-chamber PECVD system. In this paper the experimental results obtained from the degradation experiments done on two types of structures, namely pin and pinpin structures, of a-Si:H solar cells are presented.

There are four chapters in the paper. The first chapter deals with the photovoltaic effect which is described based on a simple p-n junction diode. In the second chapter the physics and the structure of hydrogenated amorphous silicon (a-Si:H) solar cells is treated. Also, some of the conditions for efficient photovoltaic energy conversion of thin film devices are briefly presented. The third chapter deals with the photovoltaic characteristics of a-Si:H solar cells. In this chapter some of the solar cell parameters, such as short-circuit current (Isc), open-circuit voltage (Voc) and fill factor (FF) are also considered. The last chapter describes the results obtained as well as the techniques used in the light- induced degradation experiments of a-Si:H solar cells.

The experimental work is done at the Research Center Julich (KFA-Julich), in the Institute of Thin Film and Ion Technology (ISI/PV), Germany.

CHAPTER ONE

The Photovoltaic Effect

Solar Cell is a solid-state or Semiconductor device (usually) which produces useful electricity in the form of a DC Voltage and Current, directly and essentially immediately from the sun's radiation via the photovoltaic effect.The photovoltaic effect is the energy conversion phenomenon involving:

. generation of free negative (electrons) and positive (holes) carries, which can move when experiencing an external force (electric field).
. Separation of the carriers by some purposely-placed inhomogeneity (e,g, a p-n junction).

In this chapter we deal with the basic concepts involved in the photovoltaic conversion of solar energy. We begin our discussion with the historical aspects of photovoltaics. Then we will describe the fundamental principles governing the photovoltaic effect. We will also discuss the photovoltaic effect based on a simple p-n junction diode which is basic to all solar cells. Finally a brief description of solar cell parameters is given.

1.1. Historical Aspects of photovoltaic.[1,2]

For over a century people have known that sunlight can produce electricity. The French physicist Edmond Becquerel discovered this fact in 1839. Like so many of his scientific contemporaries, Becquerel devoted much study to electricity. As part of a series of electricity experiments, he immersed two metal plates in a conductive fluid and exposed the apparatus to

the sun. He observed a small voltage.

In another set of experiments, Willoughby Smith discovered, in 1873, that Selenium was sensitive to light. Smith's discovery stimulated Adams and Day to conduct further tests with Selenium and light, proving that when light struck Selenium, an electrical current was generated.

In 1886, Charles Fritts came up with the first Selenium Solar cell and had ambitious plans for his cells. He predicted that they "may ere long compete with the dynamo-electric machine". Due to the compactness of the cells, he felt that each building could be its own electrical generating plant rather than be dependent on a centralized grid. The nascent Solar cell industry of the 1880s, however, never took off. Power engineers doubted that Solar cells could generate large amounts of power. No system could exist, they argued, which could generate usable amounts of energy without consuming significant quantities of material substances. Contemporary solar cell promoters could not raise theoretical arguments against these objections. The reason why solar cells work-the photovoltaic effect - lay beyond the theoretical framework of classical physics.

Only after the general acceptance of quantum mechanics which explained scientifically how solar cells produce electricity directly from sunlight - did serious interest in solar cell recommence among engineers and scientists. By the early 1930s scientists had rediscovered the selenium solar cell,renewing Fritt's dream of producing fuelless electricity for commercial purposes. Unfortunately, these new selenium cells were tied to the same low theoretical electrical output that Fritts and other early researchers faced. The 1930s also saw a revival of the interest in cuprous Oxide/copper Solar cells, but

the cells were inefficient because of the location of the action junction.

Through the early 1950s Selenium cells remained the most effective and reliable of the solar cells. The best cells could transform 1% of all incoming sunlight into electricity, hardly enough to be used as a power source. At this time, researchers at Bell Telephone Laboratories were seeking a dependable alternative energy source to power communication systems in isolated areas. Darryl Chapin, the leaders of this research team, concluded that a solar-powered device would be the ideal solution and tried to develop a more efficient Selenium cell, but to no avail.

Meanwhile, another Bell Scientist, Cal Fuller, had been exploring ways of making silicon into a more efficient rectifier. Fuller increased efficiencies by adding impurities to the silicon; When an outside voltage was applied a stronger current flow resulted. The director of the rectifier program, Gordon Pearson, fortuitously exposed one of Fuller's improved rectifiers to light. To his surprise, pearson recalled, "I noticed that It was very light sensitive". A considerable amount of electrical current was generated.

Later on Pearson brought his discovery to his friend's attention. Soon Fuller & Chapin busied themselves refining the new solar cell and found that the "rectifier" converted 4% of all incoming sunlight into electricity. Not content with the 4% conversion factor, they worked for several months trying to make the Solar cell even more efficient . By May 1954 they announced the development of a Solar cell with an efficiency of 6%.

Even though Fuller and Chapin began building cells with efficiencies as high as 15%, they were not able to make beyond a laboratory stage. It was an expensive process. Unfortunately, high-purity Silicon,costing $80 per pound, was required for efficient cells. Furthermore, a good cell had to be handcrafted. Each cell had to be sliced manually.

Just as these cells were about to be consigned to the curiosity heap, the space race resuscitated their utility. Satellites and other space Vehicles required a long term power source. In this special niche, Solar cells proved to be more competitive and cost-effective than other sources. Terrestrial applications of Solar cells, on the other hand, remained untried and unexplored since they were much more expensive than conventional sources of energy.

In the early 1970s, the disruption of oil supplies to the industrialized world led to serious consideration of photovoltaic as a terrestrial power source. This application focused research attention on improving performance, lowering costs and increasing reliability. These three issues remain important today eventhough researchers have made extraordinary progress over the years.

Nowadays there is a realization that the environment is being threatened by atmospheric pollution which results in global warming and Ozone depletion. As the source of air pollution has mostly been from the conventional energy sources, it has necessitated the search for an environment friendly source of energy. As a result the development and improvement of photovoltaic energy conversion technology has been given due importance.

1.2.Fundamental Principles

The Physics of photovoltaic effect are closely associated with the theory of diode. It is necessary, therefore, to take into account some elements of a simple p-n junction diode. A p-n junction is a specimen made of a single crystal semiconductor in which there are two adjacent regions, an n-type and p-type. The n-region is doped with donor impurities, the p-region with acceptor impurities.

When we speak of a junction, we mean the region in which the p and n regions meet. It is formed when p-type material is brought into contact with n-type martial. At the instant of junction formation, the concentration of electrons is much larger on the n side than on the p side. An analogous condition applies to the hole concentrations, which are larger on the on the p side than the n. The large difference in carrier concentrations sets up an initial diffusion current: Electrons flow from the n region into the p region, and holes flow from the p region into the n region. This flow of charge results in a region near the junction that is depleted of majority carriers - that is, of electrons on the n side and of holes on the p side. The fixed donor and acceptor impurity ions in this depletion region are no longer balanced by the free charges that were there. As a result, an internal electric field builds up with a direction that opposes further flow of electrons from the n region and holes from the p region. The magnitude of the field is such that it exactly balances the further flow of majority carriers by diffusion. The region around the junction is depleted of majority carriers, and a space - charge layer forms

in the region of high electric fields, as shown in Fig 1.1. Thus, in the absence of externally applied potentials, no current will flow.

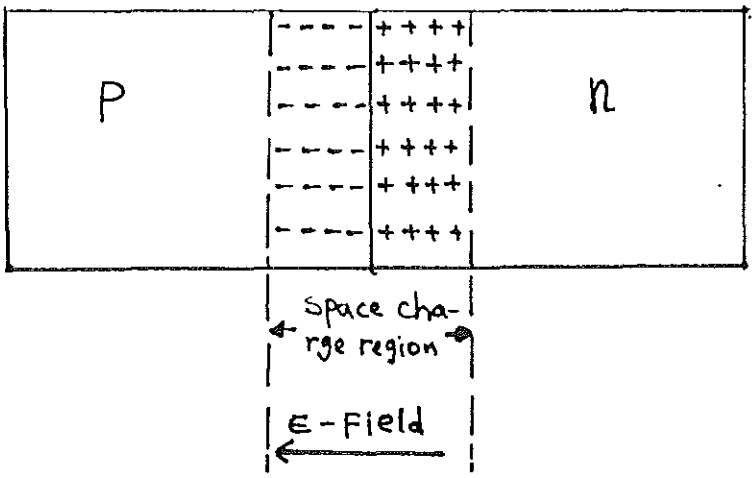

Fig.1.1 The space charge region and the electric field.

Suppose that an external voltage V is applied at the two ends of the p-n junction. A positive voltage applied to the p-side relative to the n-side encourages current flow across the junction. Conversely, a negative voltage applied to the p side relative to the n side further discourages current flow relative to the zero -voltage case. The former condition is referred to as forward bias and the latter as reverse bias. Thus, in the absence of light, the current - voltage

characteristic is given by (for detailed derivation, see Appendix A):

$$I=I_s[\exp(\frac{eV}{KT})-1] \qquad (1.1)$$

Here I is the external current flow, I_S is the reverse saturation current and V is the applied voltage. Under large negative applied voltage (reverse bias), the exponential term becomes negligible compared to 1, and I is approximately equal to $-I_S$, which is a small quantity. The rectifier action of the diode -that is, its restriction of current flow to only one direction is key to the operation of photovoltaic device.

If light is allowed to impinge on a p-n junction device, an additional photocurrent I_{ph} is produced, and the total current becomes

$$I=I_s[\exp(\frac{eV}{KT})-1]-I_{ph} \qquad (1.2)$$

1.3. Photovoltaic Effect

The production of electron hole pairs at or near a rectifying contact, by the absorption of radiation, gives rise to a photo-voltage across the contact. This phenomenon, which is called the photovoltaic effect, is best illustrated by reference to an open circuited p-n junction diode. If photons with energy $E > E_g$ are absorbed, then electron - hole pairs generated within

the depletion layer are immediately dissociated, the holes being swept by the field into the p-region and the electrons into the n-region. Those generated within a diffusion length on either side of the junction become dissociated on reaching the edges of the depletion layer, if they do not first recombine, and the minority carriers from each side are swept across to the regions where they become majority carriers. In consequence the p-region tends to develop a positive space charge and the n-region a negative space charge. This is the polarity for forward bias. Sufficient bias is built up to reduce the barrier height to a level such that a forward current, which is exactly equal and opposite to the photocurrent, I_{ph}, flows across the junction. The corresponding open circuit junction voltage V_{OC} may be obtained from the equation

$$I_{ph}=I_s\left[\exp\left(\frac{eV_{oc}}{KT}-1\right)\right] \qquad (1.3)$$

or,

$$V_{oc}=\frac{KT}{e}\ln\left(\frac{I_{ph}}{I_s}+1\right) \qquad (1.4)$$

Where the effect of internal series resistance being ignored and an ideal diode characteristic assumed.

If a load R_L is connected across the terminals of the cell the terminal voltage is reduced below V_{OC} and the current voltage

relationships can be determined from the equivalent circuit of fig. 1.2(b). The load Voltage V_L (=V) is given by IR_L and the junction current I_J is related to V_L by the usual formula i.e.

$$I_J = I_s(e^{\frac{eV}{kT}} - 1),$$

so that, since

$$I = I_s(e^{\frac{eV}{kT}} - 1) - I_{ph}$$

we have,

$$\frac{V}{R_L} = I_s(e^{\frac{eV}{KT}} - 1) - I_{ph} \qquad (1.5)$$

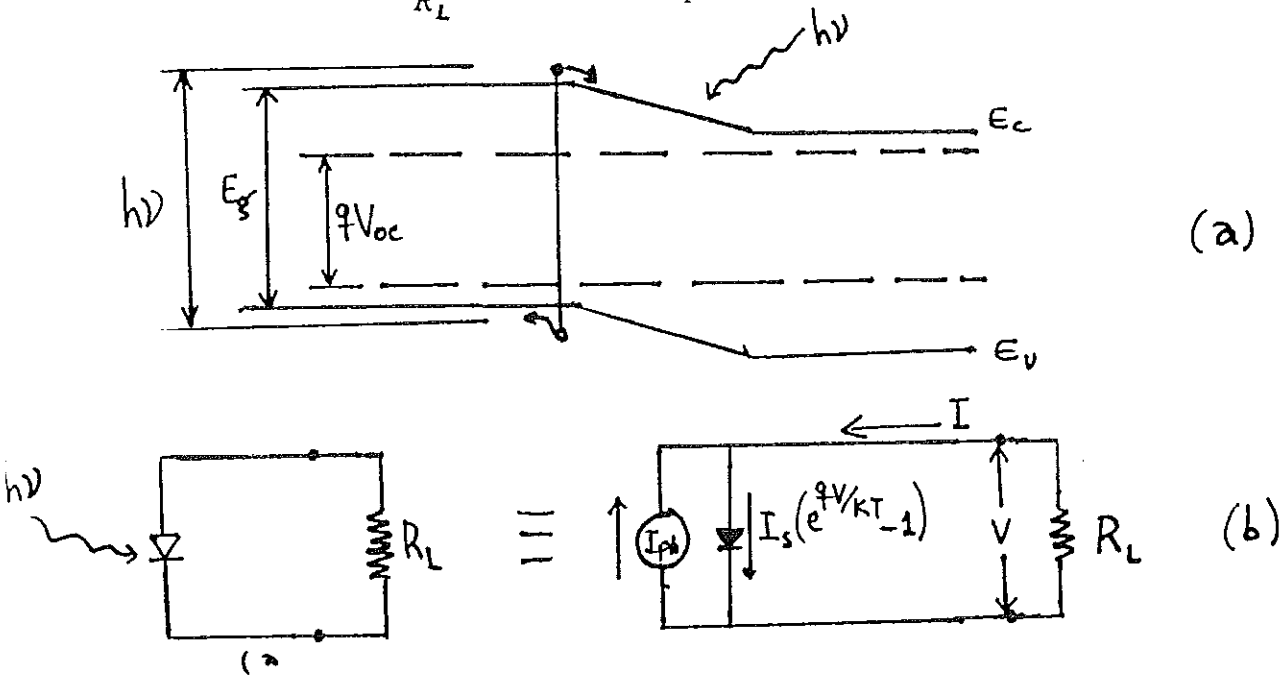

Fig.1.2 (a) Energy band diagram of a p-n junction solar cell under solar irradiation. (b) idealized equivalent circuit of a solar cell.

Eq.1.5 can be solved by numerical or graphical methods.

The I - V characteristics of a p-n junction photovoltaic cell subjected to a constant illumination is shown as curve (a) in Fig. 1.3. This characteristics is obtained by varying R_L from

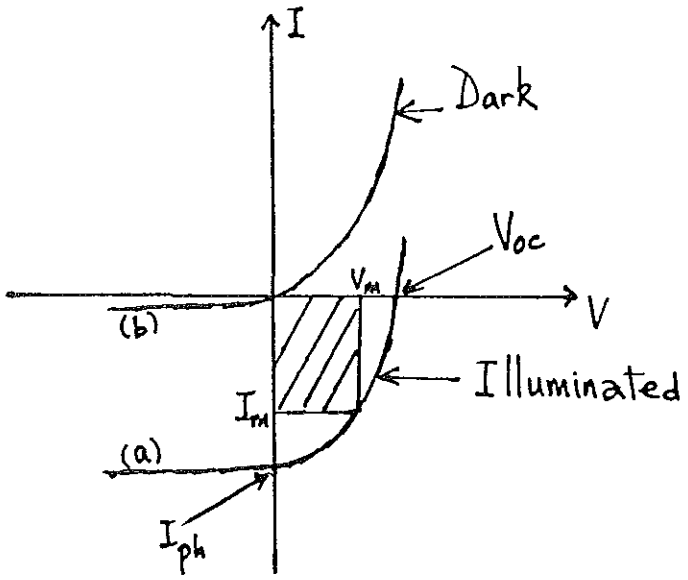

Fig 1.3 D.C. characteristic of a p-n junction photovoltaic cell (a) illuminated; (b) dark.

0 to 00 and measuring the terminal current and voltage for each value of R_L. If the load resistance is set very high (or the

load is disconnected), giving essentially infinite resistance, a voltmeter will read maximum voltage. This is called the open circuit voltage Voc. Under this condition no current is being drawn from the cell and the I-V curve (a) intercept on the abscissa axis. Conversely, if the load resistance is made zero, we will short-circuit the cell and draw the maximum possible current from the cell. This current is directly proportional to the amount of light falling on the cell and is called the short-circuit current I_{sc}(Sometimes called photocurrent, I_{ph}).Under this condition the voltage drop is zero and the I-V curve(a) intercept on the ordinate axis.

Curve(b) is the normal forward characteristic of the cell when unilluminated. It may be seen that the act of illuminating is equivalent to depression of the dark characteristic into the forth quadrant. Power can therefore be extracted from the device by operating at some point of curve(a) in this quadrant. The maximum power that can be obtained is equal to the area of the largest rectangle that can be drawn under the curve: the terminal voltage on load is clearly less than V_{oc}.

For a practical solar cell, the ideal equivalent circuit, Fig 1.2(b) should be modified to include the series resistance from ohmic loss at all contacts & surfaces (front, back, etc) and also the shunt resistance from leakage currents. The equivalent circuit is shown in Fig 1.4. If the diode current is given by the usual formula (Eq.1.2) the I-V characteristics of a practical p-n junction solar cell is found to be.

$$I = I_s\{\exp[\frac{q}{KT}(V-IR_s)]-1\}+\frac{V-IR_s}{R_{sh}}-I_{ph} \qquad (1.6)$$

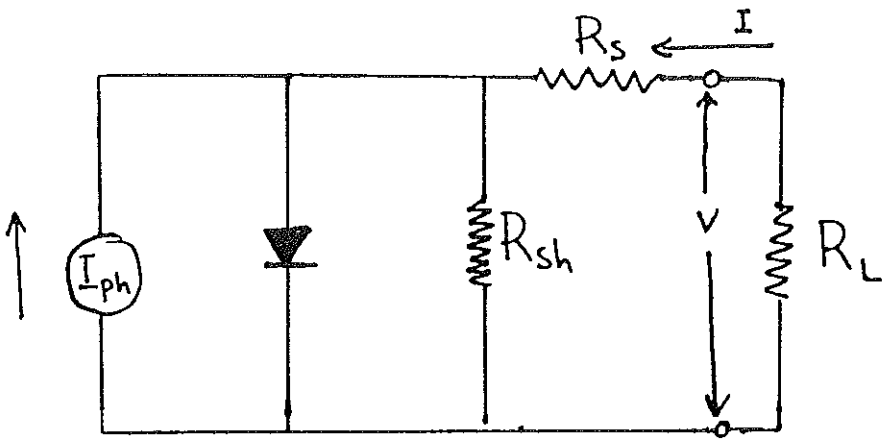

Fig. 1.4. DC equivalent circuit of a practical solar cell connected to a load R_L.

1.4 Summary of Solar Cell Parameters

Efficiency

The principal method of characterizing solar cell performance is the measurement of conversion efficiency while the cell is exposed to 1 Sun illumination (~ 100mw/cm^2). The conversion efficiency is defined as the ration of the maximum power output P_m to the incident power P_{in}, i.e

$$\eta = \frac{P_m}{P_i} \qquad (1.7)$$

Where the incident power P_i is given by

$$P_i = \int_0^\infty N(\lambda)\, \frac{hc}{\lambda}\, d\lambda \qquad (1.8)$$

Here $N(\lambda)\, d\lambda$ is the rate of arrival of photons in the range of wavelength λ to $\lambda + d\lambda$ and $\frac{hc}{\lambda}$ is the energy per photon.

Maximum Power

The power P from a solar cell is

$$P = IV = I_s V\left(e^{\frac{ev}{KT}} - 1\right) - I_{ph} V \qquad (1.9)$$

The maximum output power P_m can be determined by analytical or graphical means. Graphically, P_m can be obtained by locating the largest rectangle that can be drawn under the I-V curve. It is equal to the area of the rectangle. Analytically, the derivative of P with respect to I or V is set to zero and the result I_m and V_m determined; where I_m and V_m are the values of current and voltage, respectively, which produce the maximum

output power.

Since the dark saturation current I_S is usually negligible compared to the short-circuit current $I_{SC}(=I_{ph})$ of a solar cell and since for I=0 one has $V=V_{OC}$, one can rewrite Eq.(1.2) by eliminating I_S

$$I=I_{sc}\{\exp(\frac{e[V-V_{oc}]}{KT})-1\} \qquad (1.10)$$

The maximum power point can be obtained from Eq.(1.10) by setting d(IV)/dv =0, yielding an implicit equation for V_m :

$$V_m=V_{oc}-\frac{KT}{e}\ln(1+\frac{eV_m}{KT}) \qquad (1.11)$$

In practice V_m is approximated as

$$V_m\simeq V_{oc}-3\frac{KT}{e}.$$

Thus, Eq.(1.11) becomes

$$V_m\simeq V_{oc}-\frac{kT}{e}\ln(\frac{eV_{oc}}{kT}-2) \qquad (1.12)$$

By introducing Eq.(1.11) into Eq.(1.10), one obtains

$$I_m = I_{sc}[(1+\frac{eV_m}{KT})^{-1}-1] \qquad (1.13)$$

Which can be approximated[3] as

$$I_m = I_{sc}\frac{\frac{eV_{oc}}{kT}}{1+\frac{eV_{oc}}{KT}} \qquad (1.14)$$

The maximum out Put power P_m of the cell is then

$$P_m = I_m V_m \qquad (1.15)$$

Where I_m and V_m are obtained from Eqs.(1.14) and (1.12).

Fill Factor

Fill factor FF is defined as the actual maximum power divided by the hypothetical "power" obtained by multiplying the open-circuit voltage V_{OC} by the short-circuit current I_{SC} .

$$FF = \frac{P_m}{V_{oc}I_{sc}} = \frac{I_m V_m}{V_{oc}I_{sc}} \qquad (1.16)$$

By substituting Eq.(1.12) and (1.14) into Eq.(1.16), FF may be approximated as

$$FF \simeq \frac{eV_{oc} - KT\ln\left(\frac{eV_{oc}}{KT} - 2\right)}{eV_{oc} - KT} \qquad (1.17)$$

The maximum Out put power Pm is often expressed as

$$P_m = I_m V_m = FF\, V_{OC} I_{SC} \qquad (1.18)$$

Series and Shunt Resistance

Series resistance decreases the slope of the I-V characteristic near V_{OC}.Shunt resistance increases the slope of the I-V characteristic near I_{SC}.Both decrease P_m .

CHAPTER TWO

Hydrogenated Amorphous Silicon (a-Si:H) Solar Cells

As mentioned before, the first Silicon solar cell was made in 1954 by Chapin et al.[4] when they demonstrated that sunlight could be converted directly into electrical power with a conversion efficiency of 6% using a p-n junction single-crystal silicon. Solar cell research thrived in the early 1960s mainly as a result of the utilization of solar cells in space. Recently, the possibility of terrestrial applications has generated new interest in this area.

Since 1954 there has been a considerable progress in improving the conversion efficiency. Single-crystal silicon cells have exhibited conversion efficiencies as high as 23% while GaAs cells have exhibited conversion efficiencies as high as 25%. However, at present, the cost of these solar cells per peak watt is about 10 times expensive than the conventional sources of energy. The amorphous Semiconductor solar cell, thus, represents a promising new approach toward the development of low-cost solar cells for terrestrial applications.This chapter deals with the physics and structure of a-Si:H solar cells . First of all, the general condition for efficient photovoltaic energy conversion of thin film devices are briefly described.

2.1 Limitation of a-Si:H Solar Cells

The demonstration of photovoltaic energy conversion in a-Si:H solar cells generated a worldwide interest in this material. The reasons are obvious. The technology of a-Si:H solar cells fabricated by the glow discharge process promises low-cost fabrication of large area solar arrays on inexpensive substrate. The total material costs are very low in view of the fact that very low thickness ($\sim$ 1 μm) are sufficient for adequate device performance and the material in thin film form is deposited directly from the basic raw material, silane, thus eliminating intermediate process steps of converting the raw chemicals to si signots or si powder. Furthermore, si being abundant, availability is no problem. Moreover, the optical absorption coefficient α of a-Si:H is more than an order of magnitude larger than that of crystalline silicon over most of the visible light range. A 1-μm-thick a-Si film absorbs up to 70% of the AM1 incident radiation greater than 1.6 ev.

Even though it is considered to be a promising approach towards the development of low-cost solar cells, presently there are two factors that limit a large scale terrestrial applications of a-Si:H solar cells. They are:

(1) Low conversion efficiency.

(2) Degradation in efficiency during illumination.

Currently, there is a large effort to improve the initial conversion efficiency as well as suppressing the degradation of a-Si:H solar cells.

2.2 Conditions for Efficient Photovoltaic Energy Conversion.

The efficiency of a solar cell is according to Eq.(1.7)

$$\eta = \frac{J_m V_m}{P_i} = \frac{FF J_{sc} V_{oc}}{P_i} \qquad (2.1)$$

Where J_m and V_m are the output current density and voltage for a cell operating under maximum output power conditions and P_i is the total power incident on the cell ($P_i \sim 100 mW cm^{-2}$, for the sun directly overhead on a clear day, AM1 condition). J_{sc} is the current density of the cell under short circuit conditions, and V_{oc} is the voltage under open-circuit conditions. The fill factor (FF) is defined by Eq.(1.16), i.e,

$$FF = \frac{J_m V_m}{J_{sc} V_{oc}} \qquad (2.2)$$

We now consider the conditions that must be satisfied for a thin film device to act as an efficient solar cell. First the absorption coefficient must be sufficiently large to absorb a significant fraction of the solar energy in the thin film employed. For films of the order of $1 \mu m$ in thickness, the absorption coefficient α must be greater than 10^4 cm^{-1} over at least the visible portion of the solar spectrum. The absorption coefficient of undoped a-Si:H, for instance, is greater than $10^4 cm^{-1}$ over most of the visible light regime (1.9ev < hv < 4.0ev). Thus, an a-Si:H film need to be only $\sim 1 \mu m$ thick to meet the above conditions.

A second condition that must be satisfied is that the photogenerated electrons and holes should be efficiently collected by contacting electrodes on both sides of the

semiconductor film. This condition implies that the minority carrier diffusion length be comparable to the film thickness or that a built-in space charge field be present in most of the film.

A high performance solar cell must efficiently collect the carriers photogenerated in the active region of the device. This condition can only be met if the diffusion length l_d is greater than the thickness of the active region. For a-Si:H cells with a thickness of $\sim 0.5\mu m$, this translate into a mobility life time product ($\mu\tau$) greater than $10^{-7} cm^2/v$ ($l_d = [KT\mu\tau/q]^{1/2}$)

In most a-Si:H solar cells, a built-in electric field (E) assists in the collection of photogenerated carriers, and efficient collection occurs as long as the drift length ($\mu\tau E$) is significantly larger than the film thickness. It has been shown by Crandall (1982)[5], for instance, that the transport in a pin structure can be characterized by a collection length, $l_c = (\mu_n\tau_n + \mu_p\tau_p)E$ which is the sum of the electron and hole drift lengths. In high performance cells, the collection length is typically $\gtrsim 5\mu m$ in the short-circuit mode[6]. The collection length decreases as the cell goes into forward bias, and transport via diffusion dominates as the cell approaches the open circuit condition.

A large built-in potential (V_{bi}) across the undoped, photovoltaic active layer is also necessary for efficient photovoltaic energy conversion since this potential determines the output voltage of the cell. A built-in potential is generated by the formation of a semiconductor junction such as p-n junction, heterojunction, or pin junction. The doped layers, say p and n layers in a pin cell, are mainly responsible

for determining V_{bi}. Ideally one would want wide band gap doped layers that are degenerate or highly conductive. In such a case, the Fermi levels would lie very close to the band edges, and the built-in potential would approach the band gap. Thus, the existence of band tail states and low doping efficiency of a-Si:H are factors that limit the built-in potential in a-Si:H solar cells.

Finally, the total resistance in series with the solar cell (excluding load resistance) must be kept small so that the IR drop during operation is only a small percentage of the output voltage. Contributions to the series resistance can come from the contacts, the bulk resistivity of the semiconductor film, the sheet resistance of thin conductive coatings,the current collection grids, and the electrical wiring.

2.3 Physics and Structure of a-Si:H Solar Cells

There are various solar cell structures that have been used for making thin film cells with hydrogenated amorphous silicon (a-Si:H). These structures include Shottky-barrier cells, p-n, pin junctions and others. In this section we will deal only with pin and pinpin structures based on which we have made our light-induced degradation experiments.

2.3.1 a-Si:H pin Solar Cells

A pin diode is a p-n junction with a doping profile tailored so that an intrinsic layer, the "i-region" is sandwiched between a p layer and a n layer. Fig.2.1 shows a schematic representation of a pin diode and an energy band diagram of the junction.

When the three layers are considered independently, the energy band diagram appears as in 2.1(b). However, as one layer is deposited over another forming a pin junction, holes in the p-layer diffuse to the i-layer leaving behind a negative charge. Similarly, electrons in the n-layer diffuse into the i-layer leaving behind a positive charge. Consequently, a potential difference V_{bi} is built between the p-i and i-n junctions and the energy band diagram looks like in Fig 2.1(c). When radiation of suitable wavelength is focussed on the i-region, the hole-electron pairs which are created therein are immediately dissociated by the field across the two junctions, the holes drifting towards the p-region and the electrons towards the n-region, where they become majority carriers.

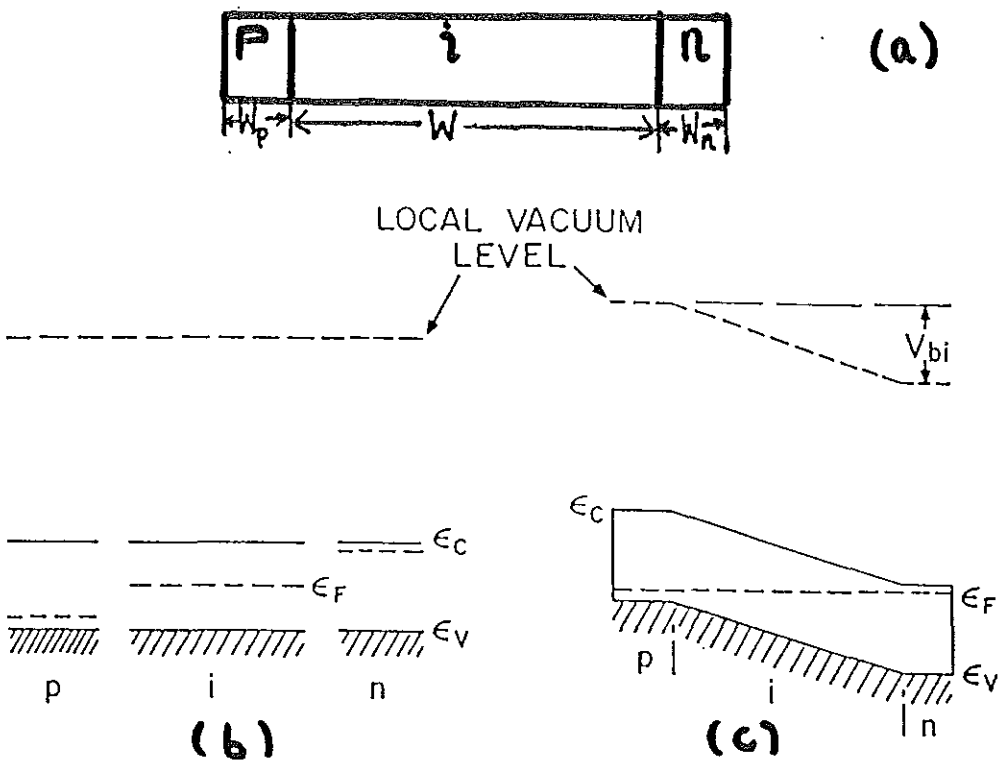

Fig 2.1 Pin diode. (a) Cross-sectional view of pin diode. (b) Energy band diagram of the three layers. (c) Energy band diagram of pin diode

The pin structure of hydrogenated amorphous silicon solar cell utilizes an undoped layer, $\sim 1\mu m$ thick, and thin p^+ and n^+ layers adjacent to the front and back electrodes. The undoped layer is grown in glow discharge in silane (SiH_4) while the p- and n- layers, which are $\sim$100-300Å thick, are usually made in a SiH_4 discharge in the atmosphere of B_2H_6 or PH_3 .

High performance (n>7%) a-Si:H can be fabricated in two types of structures[6] as shown in Fig 2.2. Type I device is fabricated by first depositing boron doped a-Si:H layer about 200Å thick on steel, followed by an undoped a-Si:H layer about 5000Å thick and finally a top phosphorous doped a-Si:H layer about 80Å thick. A 700-Å-thick indium-tinoxide (ITO) layer deposited on the top n-type layer acts as the top contact as well as an antireflection coating.

In the second type of configuration, the device is illuminated through the glass and is fabricated in the structure: glass/SnO_2/ p-i-n/Ag where the p-layer is an alloy of a-Si:C:H.

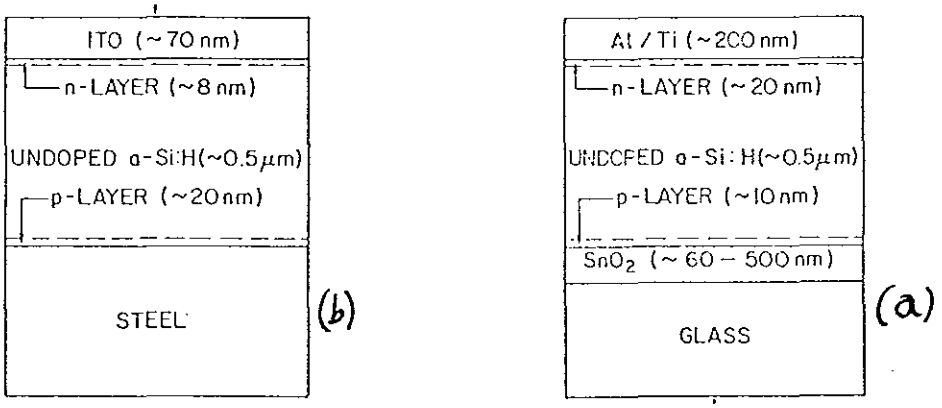

Fig 2.2 Structures of a-Si:H pin solar cells
(a) A p-i-n solar-cell structure on a glass substrate.
(b) A p-i-n solar-cell structure on a steel substrate.

We will restrict our discussion to the second type of structure, based on which we did our degradation experiments, and analyze each layer of the device.

A. Doped Layers:

One of the conditions for efficient photovoltaic energy conversion, as mentioned in section 2.2, is a large built-in potential. The doped layers, i.e p-layer and n-layer, are responsible for determining the built-in potential V_{bi} in the pin junction. This implies that V_{bi} increases with the doping efficiency of the two layers. As mentioned above, p^+ layers are formed with the addition of B_2H_6 to SiH_4 gas; however this is accompanied by a reduction in the optical band gap. Therefore, this layer is not totally suitable in a device configuration in which the junction is illuminated through the p^+ layer (as in type II) because some light is absorbed in the doped layer. Since the carrier life time in doped layers is usually very short, most of the light absorbed in this layers is lost to recombination. This absorption loss can be reduced significantly by alloying the p-layer with carbon (Pankove, 1978)[7] there by widening the band gap of the layer. This was achieved by using r.f. glow discharge in gas mixtures of SiH_4, CH_4 and H_2 and the resultant film possessed band gaps ranging from 1.76 to 2.2ev and dependent on the incorporated amount of C in the alloy. Using $(SiH_4)_{0.8}+(CH_4)_{0.2}$ ratios in the gas phase, E_g was found to be approximately 1.9ev. Secondly in all pin cells the top doped layer is thin (~10nm) in order to minimize losses due to absorption and recombination in that layer. In general, ideally one would want to make the p-layer an optical window. Since this layer is not an active layer, improving its transparency is a key for increasing the efficiency and this can

be done in two ways:(1) By reducing the thickness of the i-layer. (2) Increasing its optical gap.

The use of microcrystalline n^+ layer in the pin structure, on the other hand, has a beneficial effect in that the absorption coefficient is lowered in these films thus allowing more of the light, for instance, reflected from the back contact in Type II configurations, to enter the junction. Moreover, it is important that the device employs the thinnest n-layer consistent with electrical requirements so that optical absorption in this region could be minimized.

B. Undoped (photo-active layer).

Another factor that must be considered in the improvement of initial conversion efficiency is the thickness of an i-layer which has an optical band gap of $\sim$1.72ev for photovoltaic quality a-Si:H solar cells. As mentioned in section 2.2, the photogenerated electrons and holes must be efficiently collected for efficient photovoltaic conversion. This can be accomplished if the electric field in the i-layer, which is assumed to be uniform, is made large. Clearly the field between the two interfaces of a pin junction increases with decreasing the i-layer thickness. On the other hand, the density of photogenerated carriers increases with an increase in the i-layer thickness. Thus, an optimum thickness must be chosen for the i-layer so that high field and large optical absorption could be obtained. A typical value of i-layer thickness for efficient photovoltaic conversion in any of the above two structures (Fig.2.2) is$\sim$ 0.5μm.

C. Optical Enhancement Layers.

In any high efficiency a-Si based alloy single junction solar cells in which the device configuration is glass /SnO_2/ p-i-n/ metal with light entering from the p-side, optical enhancement plays a crucial role in determining the ultimate performance. Optical enhancement or light trapping is achieved

by scattering the incident light from the textured tin oxide film and by efficiently reflecting light back into the cell from the rear contact. The tin oxide (SnO_2) film has two important functions: (i) it acts as a window to the incoming radiation and (ii) it serves as an ohmic contact to the p-layer. The first function determines the magnitude of the short-circuit current and the second function determines, in-part, the series resistance losses and hence influences the fill factor of the device. Due to the absorption coefficient of amorphous silicon all the incident light from the solar spectrum is not absorbed in a single pass through a pin device. The degree of texture of a tin oxide enhances the optical path and hence increases the effective absorption at long wavelengths. In tin oxide films the sheet resistance, the degree of texture and the optical absorption are somewhat interdependent. In general, as the thickness increases the sheet resistance decreases, the absorption increases even though the degree of texture increases because the average grain size of the highly oriented film increases.

D. Metal Contact:

The metal contact at the back of the cell, on the other hand, serves two functions.(i) it makes an ohmic contact to the n-layer and (ii) it reflects the long wavelength light (600-

800nm), which is weakly absorbed, back into the cell. Hence, improvements in the reflectivity of the rear contact directly translate into higher wavelength response of the device. Mostly Ag is used as a back metal contact so that most of the Unabsorbed light reaching the back contact is reflected back into the photo-active layer.However, either Al or Ti(~5-10nm)/Al are more practical metal contacts that are also relatively reflective.

E. Buffer (p/i interface) layer:

Finally the last layer which plays an important role in an amorphous silicon pin solar cells is the p/i interface layer (sometimes called buffer layer). It is often found that even with a wide band gap carbide p-layer, the quantum efficiency in the blue region is lower than can be accounted for on the basis of the optical absorption in the glass, the p-and the tin oxide layers. Recombination of carriers at or near the p/i interface leads to low blue response (400-450nm) and low values of open circuit voltage. There are several possible reasons for this phenomena. Primarily, residual boron from the walls of the deposition chamber may contaminate the first few hundred angstroms of the i-layer, thereby lowering the field strength near the p/i interface. Secondly, the interface recombination at the heterojunction may increase carrier recombination near the front of the device. Thirdly, diffusion of boron from the player may contaminate the initial part of the i-layer. Thus, one method to reduce the interface recombination is to insert a thin a-SiC:H graded interface layer (known as buffer layer) between the p-and the i-layer. The effect of the buffer layer on open-circuit voltage will be discussed in the next chapter.

In general, the important technical breakthrough which contributed significantly to improve the conversion efficiency of pin type a-Si:H solar cells are:

i) application of boron-doped a-SiC:H on the window side layer
ii) improved a-SiC:H buffer layer on the p/i interface
iii) textured SnO_2 on the transparent electrode (TE) and high reflective silver film on the metal electrode.

2.3.2 a-Si:H pinpin Solar Cells

Another important structure of a-Si:H solar cell upon which we have made light induced degradation experiments is a pinpin structure (they are often called double stacked or tandem solar cell where as a pin structure is called single junction solar cell).

An important key in the practical applications of a-Si solar cell is to suppress the light induced degradation in conversion efficiency without Sacrificing the initial efficiency. As will be discussed in chapter 4, the double stacked (pinpin) amorphous silicon solar cell is the most promising to get high efficiency as well as stable operation. Fig.2.3 shows the schematic diagram of a stacked cell structure. The stacked junction structure is fabricated by growing one pin junction directly on top of another. It consists of a cell with a thinner i-layer on the transparent electrode side and a cell with a thicker i-layer on the metal electrode side. The former is called " top cell" and the latter is called "bottom cell". Both cells have a pin structure with a-Si:H for the i-layer.

In this device structure, the top cell and the bottom cell are electrically connected in series. To attain the best

performance, therefore, the current generated in the top cell must be matched to that of the bottom cell. This current matching is carried out by adjusting the i-layer thickness of the top and the bottom cells. If the current matching was properly made, the achievable initial efficiency of the pinpin solar cell could be approximately equal to that of a single junction cell with the same i-layer thickness; where the i-layer thickness of the stacked cell is defined as the sum of the i-layer thicknesses of the top and bottom cells.

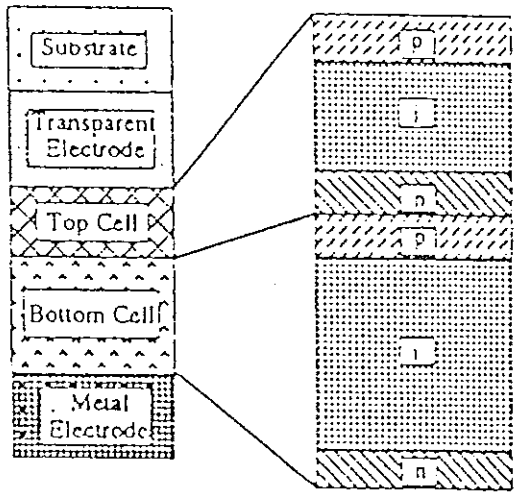

Fig 2.3 Schematic diagram of pinpin cells

If the current matching between the top cell and the bottom cell is not properly made, the difference in current between the two cells of the tandem structure would cause the accumulation of electrons in the n-layer of the top cell or holes in the p-layer of the bottom cell. This may cause neutralization of the ions, which assist in the collection of photogenerated carriers,

at the i-n or p-i junctions of the top & bottom cells, respectively. This in turn reduces the collection length and degrades the cell performance. On the other hand, since the two cells are connected in series, the voltage of the stacked cell is the sum of the individual voltage of the constituent pin cells.

As in the case of single junction cells, there are different techniques in the deposition of double-stacked solar cell that can be employed to improve the efficiency of the cell. Some of them are:

1. Insertion of high quality a-SiC:H layer as the p/i interface layer (buffer layer). The efficiency is found to be much improved if wide optical gap a-SiO:H is used to the p and p/i interface layers (Hsakai etal., 1993)[8].

2. Application of microcrystalline Si (μc-Si:H) to the n-layer of the top cell.

   The use of μc-Si:H to the n-layer of the top cell gives a good ohmic contact between the top cell and the bottom cell.

3. Use of textured electrode with an appropriate morphology.

4. Insertion of low band gap i-layer with a band gap of ~ 1.75 eV or even a wider band gap i-layer is used for the top cell. Ideally, one wants to adjust the band gap of the i-layer so that each layer produces the same photocurrent and the device efficiency is maximized.Thus, the first pin junction would employ a wide band gap (e.g 1.9ev) while the second junction would have a much smaller band gap (e.g

1.1ev). The band gaps can be tailored by using alloys such as a-SiC:H and a-SiGe:H. Either carbon or nitrogen alloying can be used to open the optical gap while alloying with tin or germanium can reduce the optical gap[6].

In a pinpin solar cell, the efficiency of the cell is also highly dependent on the i-layer thicknesses of the top and bottom cells. As experimental evidences[9] show, the solar cell parameters such as I_{sc},$V_{oc}$and FF are affected by the variation of the top and bottom i-layer thicknesses. Fig.2.4 and Fig.2.5[6] show the variation of the cell parameters (measured under AM1.5, 100mw/cm^2, 25^{o}c) at various i_1 and i_2 layer thickness combinations, where i_1 and i_2 are the i-layer thicknesses of the top cell and bottom cell, respectively.

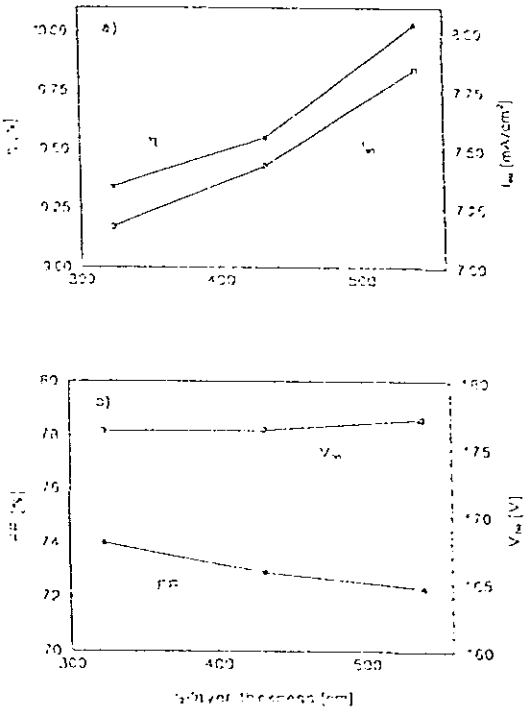

Figure 2.4
a) Efficiency η and short circuit current density I_{sc} and b) fill factor FF and open-circuit voltage V_{oc} as function of i_2 for constant i_1 layer thickness (60 nm)

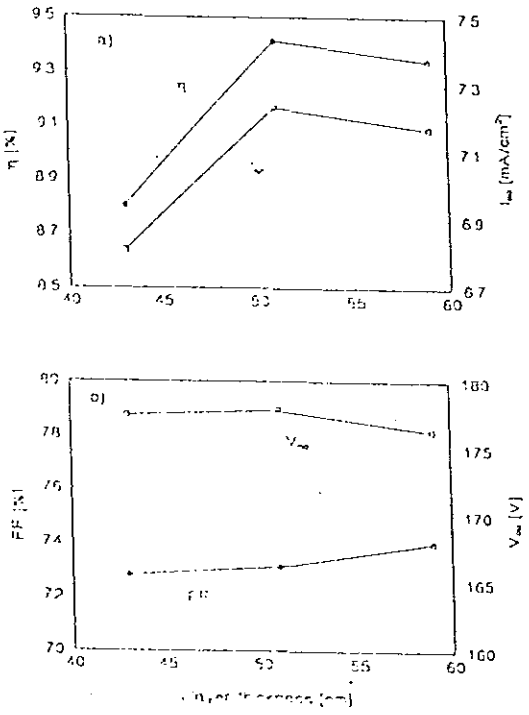

Figure 2.5
a) Efficiency η and short circuit current density I_{sc} and b) fill factor FF and open-circuit voltage V_{oc} as function of i_1 for constant i_2 layer thickness (325 nm)

As can be seen in Fig.2.4, the efficiency of the cell increases with increasing i_2 layer thickness (i_1=60nm), which is mainly due to an increase of I_{SC}. Fig.2.5 shows that there is a maximum in efficiency, due to a maximum in I_{SC}, when varying the i_1 layer thickness (i_2=325nm). The highest initial efficiency was obtained with the maximum i_1 and i_2. On the other hand, as will be discussed later, the degradation of stacked cells also increases with an increase of the i-layer thickness. Thus, one must take into account these factors in designing the i-layer thickness of a stacked cell to obtain a high stabilized efficiency.

CHAPTER THREE

Photovoltaic Characteristics of Hydrogenated Amorphous Silicon (a-Si:H) Solar Cells

In the last chapter we have discussed the structures of hydrogenated amorphous silicon (a-Si:H) solar cells and considered, specifically, pin and pinpin structures of a-Si:H solar cells. This chapter will deal with the photovoltaic characteristics and some important parameters of these devices. First, current-voltage behaviour of a-Si:H solar cell is described. Then, solar cell parameter such as short-circuit current (Isc), open-circuit Voltage (Voc), and fill factor (FF) are discussed. Finally, the influence of some parameters (temperature, pressure, impurities) during deposition on the photovoltaic properties of a-Si:H is briefly presented.

3.1 Current-Voltage (I-V) Behaviour of a-Si:H solar cells.

3.1.1 Dark I-V characteristics

As it is well known, the current density J_d of a diode in the dark is generally expressed by the sum of the diffusion current density J_{diff} and the recombination current density J_{rec} as follows:

$$J_d = J_{diff} + J_{rec} \qquad (3.1)$$

However, experimental evidences[10] show that the dark current is mainly due to the recombination current in a-si based pin

diodes and is given by

$$J=J_s[\exp(\frac{qv}{nKT})-1] \qquad (3.2) \qquad (4.2)$$

Where Js is the reverse saturation current density and n is the diode quality factor. A representative, dark current-voltage characteristics of a 1 cm^2 Pin junction a-Si:H solar cell measured at 25^oc is shown in Fig.3.1. The detail of measurement technique will be described in the next chapter.

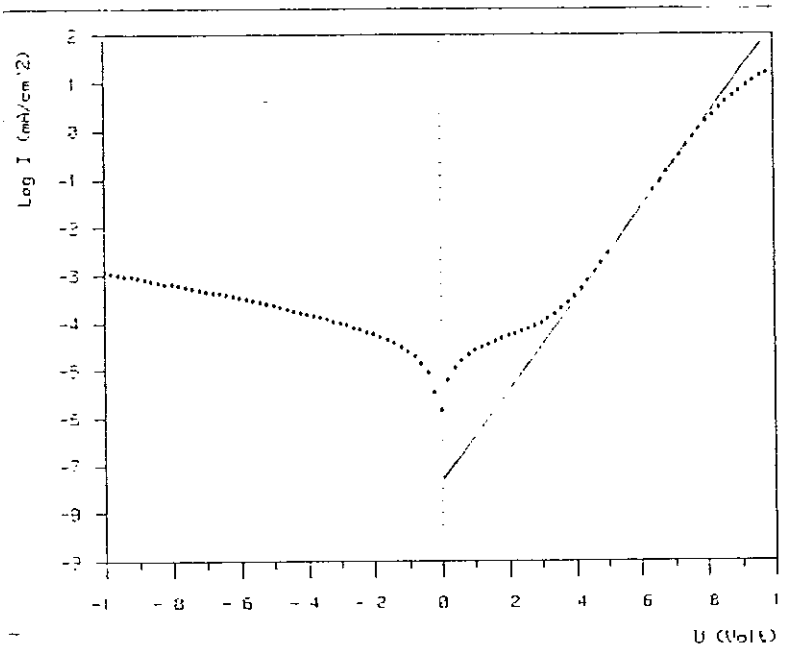

Fig.3.1. Dark I-V characteristics of a pin cell with structure glass/SnO_2/P(a-Si:C:H) -i-n/Ag and area=1 cm^2 at 25^oc . The intercept of the straight line shown is J_S.(KFA/ISI-PV,Germany, 1993).

Sometimes it is possible to characterize the performance of a cell by its reverse saturation current density (Js) and its diode quality factor (n). Relatively efficient a-Si:H cells

typically exhibit[6] values of Js in the range of 10^{-12} to 10^{-11} A/cm^2 and diode quality factors of ~ 1.5 - 1.8. The value of the diode factor n is often approximated from the dark I-V curve by taking a slope of the curve which is plotted on a semi logarithmic axis. Also, the magnitude of saturation current is approximated by locating the value of J at V=0. However, due to limited resolution of a measuring instrument, the reverse saturation current is often estimated by extending the straight line, which is used to determine the slope of the dark I-V curve, so that it crosses a point on the abscissa.

3.1.2. Light I-V characteristics

The light I-V characteristics of the same cell measured under standard conditions is shown in Fig.3.2. The standard test conditions (STC) [11] for characterizing solar cell performance are: (1) reference solar spectral irradiance distribution (AM 1.5 (AM = air mass); (2) irradiance (integrated over all wave lengths) $\bar{E}_{AM1.5}$ E_{STC}= 1000Wm^{-2};(3) temperature of the cell of 25^{o}c

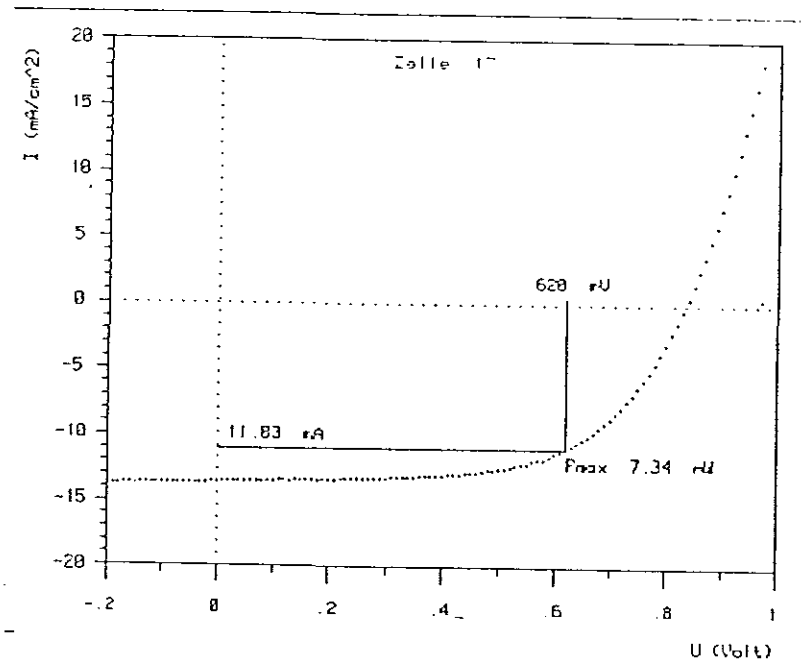

Fig.3.2. Light I-V characteristics of a Pin cell at 25^{o}c (KFA/ISI-PV, 1993)

From the light I-V characteristics several solar cell paramters, such as , FF, V_{OC}, I_{SC}, R_S and R_{Sh} can be determined. V_{OC} and I_{SC} are obtained from the curve simply by locating those points of the I-V curve that crosses the abscissa & ordinate respectively. FF is determined by finding the current and voltage at the maximum power point (I_m & V_m, respectively) from the curve and by dividing the maximum power output (I_mV_m) to the product of I_{SC} and V_{OC}. Finally, the values of R_S and R_{Sh} are often approximated from the slope of the curve at $V=V_{OC}$ and at $V=0$, respectivly.

The I-V characteristics of the best single junction and stacked cells prepared in KFA/ISI-PV (1993) are shown in Fig. 3.3 (a) and (b)[9]. The stacked cell V_{OC} of 1770 $\pm$ 10mv approaches the sum of the individual V_{OC} of the constituent pin cells: 920 $\pm$ 5mV for the top cell, and 870 $\pm$ 5mv for the bottom cell. The efficiency of the best stacked cell prepared in the group is only a little lower than the best single junction cell of the group.

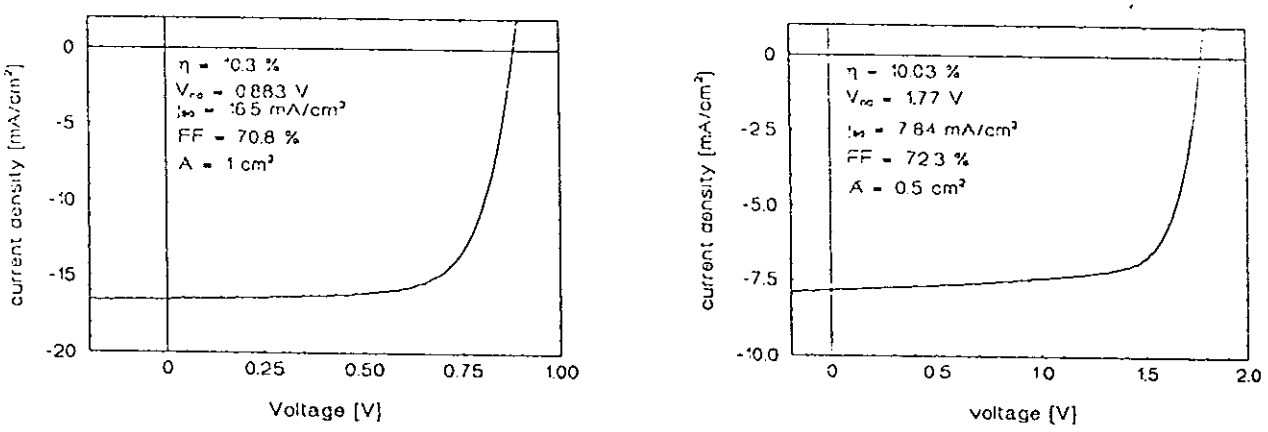

Fig.3.3. Comparision of light I-V characteristics (AM1.5,25^{o}c). (a) single junction,(b) stacked cell.

3.2 Solar Cell Parameters

In this section some points on the most important parameters of hydrogenated amorphous silicon (a-Si:H) solar cells, i.e I_{SC}, V_{OC} and FF will be presented.

3.2.1. Short-circuit current, Isc

Efficient photovoltaic conversion, discussed in chapter 2, requires the generation of large-short-circuit currents, I_{SC}, and open circuit voltage, V_{OC}, and also the ability of the cell to supply power to a load. For large value of J_{SC}, the primary requirement is the absorption of a significant fraction of energy of sunlight to create electron-hole pairs in the cell. For this purpose the matching of the optical gap of the photovoltaic active region to the solar spectrum is necessary. As was discussed in the last chapter, ideally one would like to tailor the structure of the solar cell so that a large portion of the solar spectrum can be absorbed in the undoped layer of the diode. However, experience shows that for a-Si:H produced by glow - discharge in silane, samples having the "best" semiconductor properties (low density of states in the gap, large photoconductivity, etc.) have an optical gap of around 1.7 eV. That means the material is practically transparent to photons below 1.65 eV so that a large part of the solar spectrum is lost. This results in a rather small short circuit current, typically smaller than 16 mA/cm^2 which is to be compared to a value of more than $32mA/cm^2$ for the best silicon crystal diode.

From the above discussion one may expect to increase J_{SC} by decreasing the optical gap. Also, increasing the thickness of the undoped layer of the junction increases the number of

photons absorbed in the cell per unit time. Ofcourse, in principle, one could almost double the short-circuit current by moderate decrease of the optical gap from 1.8 eV to 1.4 eV. However, in practice, the most important parameter for efficient collection of the photogenerated carriers, i.e, collection length lc ($l_c=[\mu_n \tau_n + \mu_p \tau_p]$ E where μ and τ are mobilities & lifetime of carriers and E is electric field), decreases when the optical gap becomes smaller than 1.7 eV[10]. Greater collection lengths have been strongly correlated with a decrease in the density of states (DOS) in the gap, i.e with the quality of the material. Thus, a small-gap material, having good photovoltaic properties, still remains to be the subject of material research activities in many laboratories in the world. Recently, K.chang Park et al., 1991[11], have been successful in manufacturing a low defect density, low band gap (between 1.6 and 1.65 eV) amorphous Silicon (a-Si).

On the other hand, the collection length also increases with the magnitude of the built- in electric field in the photodiode. Since the latter is inversely proportional to thickness, the diode should have the minimum thickness compatible with an acceptable absorption of the solar light. Based on this consideration the optimum thickness for a-Si:H solar cells is between 0.3 and 0.6μm. Usually 5000Å is used for the i-layer thickness in a single junction a-Si:H Solar cells.

Generally, the a-Si:H solar cells exhibit built-in potentials of the order of 1 Volt, and since the film thickness is ~1μm, fields of ~10^4 V cm^{-1} are present. The large optical absorption of a-Si:H causes an appreciable density of electron-hole pairs to be generated in the photovoltaic active region. These photogenerated pairs are separated by the electric field in the junction and are then collected by the cell electrodes.

The photocurrent collected in the external circuit of a solar cell is thus the sum of the extracted electron and hole pairs.

3.2.2. Open Circuit Voltage, Voc

For further improvement in conversion efficiency of a-si based pin solar cells, the open circuit voltage Voc is the most feasible parameter in the photovoltaic characteristic. One of the effective approaches to increase the Voc is inserting an intrinsic a-SiC interface (called the buffer layer) at the p(a-SiC)/i(a-Si) interface. The role of inserting this layer can be well understood by investigating the dark I-V characteristics of a solar cell.

As has been mentioned, the dark current density J_d is expressed by the sum of the diffusion current J_{diff} and the recombination current J_{rec} as

$$J_d(V) = J_{diff}(V) + J_{rec}(V) \qquad (3.3)$$

The recombination current J_{rec} is considered to consist of two components; one is related to the recombination in the bulk region and the other is related to the recombination in p/i interface region as follows:

$$J_d(V) = J_{diff}(V) + \overset{b}{J}_{rec}(V) + \overset{int}{J}_{rec}(V) \qquad (3.4)$$

Where $J^{b}_{rec}(V)$ is the recombination current in the bulk region and $J_{rec}{}^{int}(V)$ the recombination current in the p/i interface region.

It is observed experimentally[12] that the dark current under the forward bias condition is mainly due to the recombination at the p/i interface region. The study on the effect of i-layer thickness on the dark I-V curve shows that the contribution to the dark current from bulk recombination is negligible in the cells with a thin i-layer (<2000Å) thickness. In the conventional diode, the current due to the carrier recombination in the bulk of the i-layer is given by

$$\underset{rec}{J^{b}} = \underset{s}{J^{b}} \exp\left(\frac{qV}{2kT}\right) \qquad (3.5)$$

$$J_s^{b} = qN_i W(i)/2\tau \qquad (3.6)$$

Where N_i is the intrinsic carrier density, τ is the effective life time of carriers in the depletion region and W(i) is the thickness of i-layer. Consequently, if the dark current is governed by this recombination mechanism, it should be approximately proportional to the thickness of the i-layer. However, experimental evidence[12] reveals that the recombination in the bulk has a significant contribution for the dark current only in the cells with thicker i-layer (>2000Å) or with low quality i-layer (a-SiC:H film with $E_g(i) > 1.95$ eV, $E_g(i)$ is the band gap of the i-layer). In these cells, the dark I-V curve is governed by the J_{rec}^{b} because of an increased dangling bond density in the i-layer; an increase in the dangling bond corresponds to reduction in the life time in Eq.(3.6), and then results in increase in J_s.

On the other hand, the contribution of diffusion current to the dark current is also negligible. This is because as it was observed experimentally[12], the saturation current J_s decreases with increasing $E_g(i)$. If the current were governed by the

diffusion current, the satuaration current should be kept constant independent of the $E_g(i)$. Hence this result indicates that the diffusion current J_{diff} is not predominant in the dark current.

The principal path of the dark current is, therefore, neither the diffusion nor the recombination in the bulk. The most possible path is, thus, considered to be recombination at the p/i interface. Of course, there are two interfaces in a pin junction diode -p/i interface and n/i interface. But the dark current arises only from recombination at the p/i interface/ This was observed[12] by inserting constant band gap interface layer (buffer layer) at the p/i and n/i interfaces The dark I-V curve of solar cells was found to be shifted only when a buffer layer was inserted at the p/i interface. Before discussing the role of this layer to improve the open-circuit Voltage, let us first analyze the influence of dark current on the V_{oc}.

In general, the dark curent density J_d of a-si based Pin solar cells, which is dominated by the recombination current at the p/i interface region J_{rec}^{int} is, expressed as

$$J_d = \overset{int}{\underset{rec}{J}} = J_s \exp\left(\frac{qV}{nkT} - 1\right) \qquad (3.7)$$

Where J_S is the current density at V=O extrapolated from the slope of log (J_d)-V plot; n is the diode quality factor, k is the Boltzmann's constant and T is the temperature. On the other hand, applying a simplified model, the J-V characteristics of solar cell under illumination is expressed as

$$J=J_s[\exp(\frac{qV}{nKT})-1]-J_{sc} \qquad (3.8)$$

where J_{sc} is the short circuit current density.

At $V=V_{oc}, J=0$. Thus we have,

$$V_{oc}=\frac{nkT}{q}\ln(\frac{J_{sc}}{J_s}+1)\approx\frac{nKT}{q}\ln(\frac{J_{sc}}{J_s}) \qquad (3.9)$$

Hence for a given J_{sc}, the open circuit voltage increases logarithmically with decreasing saturation current. Suppression of the reverse saturation current is, therefore, the major step towards the improvement of the V_{oc} of the cell. This is accomplished by inserting a buffer layer at the p/i interface.

As mentioned above, inserting a buffer layer at the p/i interface shifts the dark J_d - V curve of the cell . For a better understanding of this feature, the dark J_d- V characteristics of cells with p/i interface layer, as was obtained by T.Yoshida et al., 1988[12], is plotted in Fig 3.4.

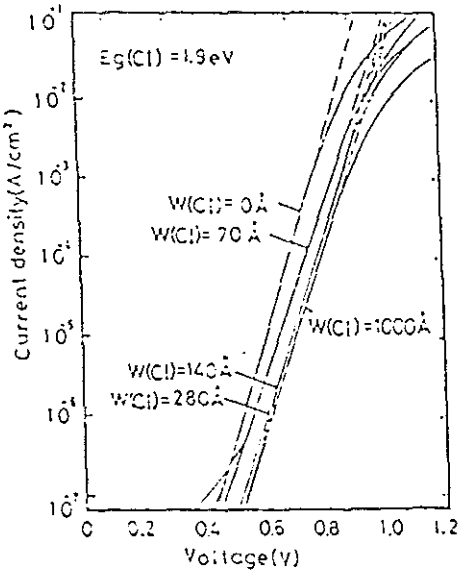

Fig.3.4. J_d-V curve of cells with p/i buffer layer for W(CI)=0, 70,140,280,1000A, where W(CI) is thickness of buffer layer. The sum of buffer layer and i-layer were fixed at 1000Å.

As can be seen in the plot, the dark J_d-V curve is shifted to the right when buffer layers of different thicknesses are incorporated into the p/i interface. Thus, we see that for a particular voltage the value of J_d decreases with the increase of thickness, W(CI), of the buffer layer. This means that with the increase of W(CI), the value of reverse saturation current J_s is reduced. Consequently, the open circuit voltage of the cell is improved.

Another important point that must be noted from the J_d-V curve (Fig 3.4) is that it is not considerably moved for W(CI) > 140Å. This led to a generalization[12] that the current transport of solar cells with the p/i buffer layer which is thicker than 140Å is effectively the same as that of the same cell in which the band gap of the whole i-layer is equal to that of the buffer layer.

For cells with i-layer thicknesses > 2000Å or with low quality i-layer, the current due to recombination in the bulk can not be neglected. Thus, the open-circuit voltage of solar cell parameters can be improved by insertion of a buffer layer

at the p/i interface with a thickness greater than 100Å and by reducing the i-layer thickness to minimize dark current.

Before closing the discussion on the behaviour of V_{OC}, let us mention some points on the temperature dependence of open-circuit voltage. From Eq.(3.9) it is clear that the open-circuit voltage increases logarithmically with decreasing a saturation current J_S. The saturation current, on the other hand, dependens exponentially on temperature as can be seen from the relation derived for a simple p-n junction (see Appendex A).

$$J_s=qn_i^2\left[\frac{D_n}{N_aL_n\tanh(W_p/L_n)}+\frac{D_p}{N_dL_p\tanh(W_n/L_p)}\right] \qquad (3.10)$$

Since

$$n_i^2=N_cN_o\exp(-E_g/kT)$$

Eq.(3.10) can be written as

$$J_s=J_{so}\exp\left(-\frac{E_g}{kT}\right) \qquad (3.11)$$

Where

$$J_{so}=qN_cN_o\left[\frac{D_n}{N_aL_n\tanh(W_p/L_n)}+\frac{D_p}{N_dL_p\tanh(W_n/L_p)}\right] \qquad (3.12)$$

is constant.

N_C and N_V are the density of states in the conduction and

valence bands, respectively. D_n & D_p are electron and hole diffusion coefficients; L_n and L_p are diffusion length of electrons & holes; W_p and W_n are the thicknesses of the p and n regions. N_a and N_d are the concentration of acceptor & donors.

Assuming a similar expression (Eq.3.11) holds for a Pin junction diode (of course, with different expression for J_{so}) the open-circuit voltage V_{oc} may be expressed as:

$$V_{oc} \approx \frac{nkT}{q} \ln \left[\frac{J_{sc}}{J_{so} \exp\left(-\frac{E_g}{kT}\right)} \right] \qquad (3.13)$$

Or,

$$V_{oc} \approx \frac{nE_g}{q} - \frac{nKT}{q} \ln \frac{J_{so}}{J_{sc}} \qquad (3.14)$$

From Eq.3.14, we clearly see that the open-circuit voltage V_{oc} decreases linearily with an increase in temperature. on the other hand, unlike the short-circuit current I_{sc}, the V_{oc} increases with an increase in the band gap.

In general, the current-voltage characteristics of a-Si based Pin solar cells and the role of the buffer layer can be summarized as follows [12]:

1) The current-voltage characteristics under dark condition is dominated by the recombination current at the p/i interface region and the effective thickness of this interface region is about 100Å.

2) Insertion of a buffer layer with a thickness of more than 100Å is equivalent to an increase of the band gap of the whole i-layer to that of the buffer layer.

3.2.3. Fill Factor,FF

The fill factor FF is considered to be a measure of the "squareness" of an I-V curve. It was mentioned before that R_S and R_{Sh}affect the slope of an I-V curve at $V=V_{OC}$and $V=0$, respectively, i.e, at the open-circuit and short-circuit Values. As the series resistance R_S of the cell increases from an ideal value (i.e, $R_S=0$) and/or the shunt resistance R_{Sh} of the cell decreases from an ideal value ($R_{Sh}=\infty$), the I-V curve of the cell becomes more "round" than "square" reflecting a decrease in fill factor.

Generally, in order to improve the efficiency of a solar cell one must optimize the three parameters discussed in this section (I_{SC},$V_{OC}$and FF). The challenge of this work lies in optimizing the three of them altogether.

3.3 Effects of Deposition Parameters on the Photovoltaic Properties of a-Si:H Solar cells

One of the efforts in the production of hydrogenated amorphous silicon solar cells is deposition of devices which have the best semiconductor properties, such as low density of states in the gap, large photoconductivity, etc. The photovoltaic properties of solar cells are determined by the quality of the semiconductor obtained during deposition. Some of the parameters that influence the photovoltaic properties of a-Si:H solar cells are substrate temperature, pressure of

the gas, impurities and others. Here we will briefly discuss the effect of these parameters.

3.3.1. Effect of Substrate Temperature

The photovoltaic properties of a-Si:H solar cells are strongly influenced by the substrate temperature (T_S) during deposition. For substrate temperatures $\lesssim 200^{o}$c the devices exhibit poor photovoltaic properties due to large defect densities. Consequently, other electronic properties such as photoconductivity and photoluminescence are also adversely affected by the short recombination. It has been shown by Lucovsky et al. (1979)[13] that films produced at low T_S generally contain hydrogen concentrations in excess of 30%, in which case the material can be described as a polymeric type structure containing an excess of (SiH_2) and (SiH_3) chains. Thus, the defects formed in a-Si:H at substrate temperatures $\lesssim 200^{o}$c may be associated with dihydride or trihydride groups. Although the H/Si content ratio within the film, and the consequent optical band gap Eg is reduced when T_S is increased it is the mode of incorporation of H into the Si matrix that appears to have a major effect on the electron behaviour. Thus, it is the fundamental change from a polymeric type structure for samples deposited at low temperature to a monohydride at higher T_S, that has a major effect on the reduction of the density of states in the gap.

Poor photovoltaic properties are also obtained when the substrate temperature is > 400^{o}c. In this case, the defects are dangling bonds left behind as the hydrogen atoms diffuse out of the film. Due to the presence of large defect densities as $T_S > 400$ °c, the electron-hole pairs created during illumination are lost by recombination or being trapped

before they are efficiently collected by the electrodes of the cell. Thus, the value of J_{SC} decreases as T_S increases above 400°c. Also, the FF drops rapidly as the effective series resistance of the cell increases.

Efficient a-Si:H solar cells can only be made in the range of substrate temperatures between 200 and 400°c. This range encompasses the minimum defect density as shown by D.E. Carlson et. al (1985)[6]. As T_S increases from 200 to 400 °c, J_{SC} increases and V_{OC} generally decreases. The increase in J_{SC} with T_S is due to the decrease in Eopt and increase in absorption coefficients and also due to the enhancement in carrier recombination lifetime. The decrease of V_{OC} as T_S increases may be associated with the dependence of built-in potential (V_{bi}) on E_{opt}

3.3.2. Pressure of the Gas

The pressure of the gases during deposition affects the properties of the film, since gas phase polymerization is encouraged at high pressures (Brodsky, 1977)[13] with the consequence that SiH_2 and SiH_3 grouping within the film becomes more pronounced.

3.3.3. Impurities

Another factor that influence the photovoltaic properties of a-Si:H solar cells during deposition is impurities normally found in the glow discharge environment. Impurities can create defect levels in the gap of a-Si:H. The most common impurities are Oxygen, Carbon and Nitrogen with concentrations typically in the range of 10^{18}- $10^{20}cm^{-3}$ (Magee and carlson, 1980)[14].

The effect of impurities on solar cells has been investigated by deliberately adding gases such as H_2O, N_2, and CH_4 to the SiH_4 discharge during the deposition of a-Si:H (Carlson, 1982a)[15]. Cellefficiency was reduced by ~15-30% by adding either ~0.2% H_2O or ~1% N_2 or ~10% CH_4 to the SiH_4 discharge. Delahoy and Griffith (1981)[16] found that the presence of both oxygen and nitrogen in the SiH_4 causes a greater reduction in solar cell efficiency than caused by the presence of either gas by itself. This synergistic effect suggests that some of the recombination centers are nitrogen - oxygen complexes, and defects such as NO_2 have been observed by electron spin resonance in X-irradiated a-Si:H films (Pontuschka et al. , 1982)[17].

CHAPTER FOUR

Influence of Controlled Light-Induced Degradation on a-Si:H Solar Cell Parameters.

4.1. Introduction

During the past few years, amorphous silicon alloys have become the leading candidate for low cost solar cells and large area displays. However, there are two unresolved problems associated with a-Si based solar cells for large scale applications. One of the central techonological obstacles is the low conversion efficiency of the cells. Many researchers have, therefore, used different techniques towards the advancement of the initial conversion efficiency. Accordingly, in the last 12 years, a-Si:H research cells have improved steadily from about 2.5% to greater than 12% [18].The other obstacle for large scale technological application of a-Si solar cells is a degradation of critical material properties with exposure to light. It has been found that amorphous silicon cells will degrade, i.e., the initial efficiency will be reduced by a considerable fraction, when subjected to operational conditions. What is needed is high stabilized efficiency at low cost.

So far we have been discussing ways of increasing the initial conversion efficiency of a-Si:H solar cells. We considered different parameters that would improve the performance of amorphous silicon solar cells. Although some progresses have been achieved in the last few years in improving the initial efficiency, further research is required to achieve stable, high efficiency a-Si:H solar cells. Thus, improving only the initial conversion efficiency is not

sufficient without reducing the loss in efficiency. To meet this goal, different investigations are being made in many laboratories on the stability of a-Si:H solar cells together with an effort towards high efficiency.

One of the major steps towards the suppression of light-induced degradation of a-Si solar cells is understanding the degradation behaviour of solar cell performance. In this chapter we will describe the experiment that has been done to study the influence of light-induced degradation on the performance of a-Si:H solar cells. Before describing the experimental details, let us begin with the basic principles governing light-induced degradation of a-Si:H solar cells.

4.2. Staebler-Wronski Effect

It was found that when a-Si:H solar cells are subjected to illumination, the performance of the cells is changed through the creation of recombination centers and charged traps[19].These light-induced centers are metastable and can be annealed out. The observation of metastable changes in a-Si:H goes back to the work of Staebler and Wronski[20],who found in 1977 that the dark conductivity and photoconductivity of glow-discharge-deposited amorphous silicon can be reduced significantly by prolonged illumination with intense light. The observed changes were found to be reversible by annealing the a-Si:H samples at elivated temperatures (> 150^{o}c), and were attributed to a reversible increase of the density of gap states acting as recombination centers for photoexcited carriers and leading to a shift of the dark Fermi level E_F toward midgap. Since this first report, light-induced metastable changes in the properties of hydrogenated amorphous silicon are referred to by the name Staebler-Wronski effect

(SWE) and have been studied quite intensively by many researchers.

The result of different authors agree qualitatively in that illumination with intense light leads to the creation of additional metastable states in the gap of amorphous silicon which influence its electronic and optical properties by decreasing the life time of excess carriers and shifting the position of the dark Fermi level in a reversible manner. The quantitative conclusions from the different experiments, however, do not agree at all. Discrepancies exist as to the absolute density of the metastable defects (Staebler and Wronski suggested 10^{18}defects/cm^3), there position in the mobility gap, and whether one or more types of defects can be created by illumination. Another important question that has remained unanswered until now is whether the SWE is mainly related to the bulk or to the surface (or interface) properties of a given a-Si:H sample. At present, experimental evidences exist for either of the two extreme interpretations as well as for models considering reversible changes both in the bulk and the surface density of states.

Despite the extensive experimental efforts in understanding the SWE, no conclusive picture of the phenomenon has emerged so far. Even basic questions are still the subject of controversial discussion, e.g., whether the SWE is caused by impurities, whether one or more species of metastable defect exist, or whether actually new defects are created at all during illumination, rather than the charge state of already existing defects being changed predominantly by electronic process.

Based on several experimental results a number of

microscopic processes have been proposed to explain the SWE. The first one involves the separation of weak Si-Si bonds into one or two Si dangling bonds and is, therefore, known as the "bond breaking model". This mechanism, together with a possible rearrangement of hydrogen atoms in a-Si:H, has been put forward by a number of researchers[20,21]. A different picture of the SWE involves reversible changes in the charge or hybridization state of already existing dangling bonds. Finally, there has been some experimantal evidences that the magnitude of the SWE increases with the concentration of impurities like oxygen, nitrogen, or carbon in a-Si:H. This observation has led to a model according to which the SWE is not intrinsic to a-Si:H, but rather linked to the presence of impurities in special microscopic configurations.

Though there are a number of defect creation models, it is generally accepted that the non-radiative recombination of excess carriers is responsible for the creation of metastable defects in a-Si, independent of whether the excess carriers are created by illumination or, for instance, by double injection in a forward biased p-i-p diode. Obviously, during illumination of a-Si:H solar cells the defects are created by the recombination of photo-generated carriers.

In general, the light-induced metastable changes in a-Si:H films, i.e., S-W effect is attributed to the increase in defect density. The increase in defect density causes a reduction in the carrier life times and leads to the degradation in the characteristics of a-Si:H solar cells.For instance, the decrease in carrier life time can cause degradation even when the internal electric field remains relatively uniform since the photocurrent decreases as $\mu\tau$ (or l_c) decreases; the effect of decreasing collection length

on fill factor is clearly seen in Fig.4.1.

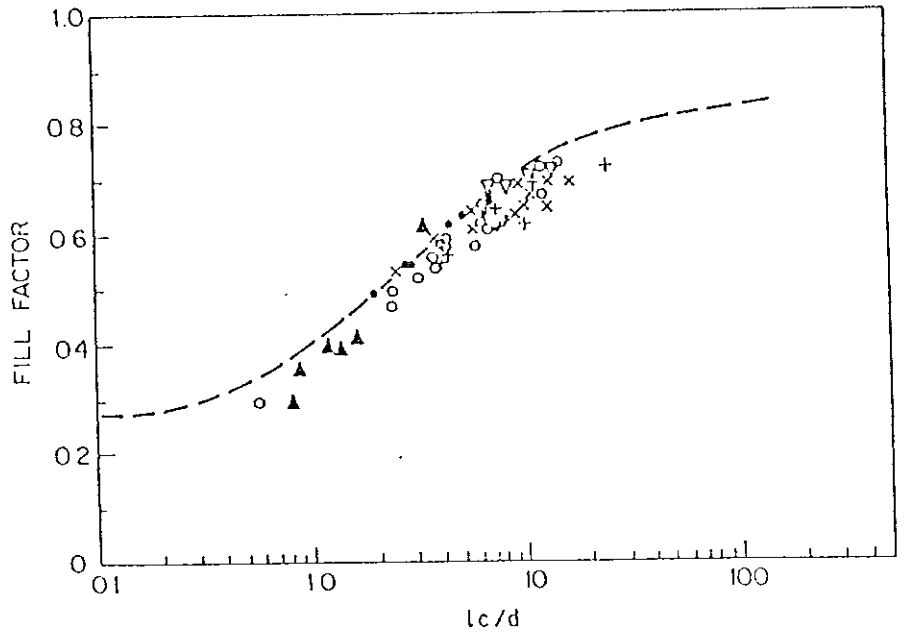

Fig.4.1 Fill factor as a function of collection length[6].

Regardless of the debates on the origin of defect generation, Redfield and Bube[22] attempted to describe the degradation process using simple differential rate equation based on several principles. The first principle is that transitions between two states of metastable center must be reversible, whether they are driven by thermal energy or by light. The second principle used is that there must be a maximum in the density of metastable defects because there is a finite number of centers from which they arise. Let N_T be the total density of these defects. This N_T is divided between the density of actual defects N and the density of latent defects N_L. In conventional terms N is the density of broken bonds and N_L is the density of "weak", but inactive bonds, the only observable is N, so all the analysis is directed to it.

A third principle is that the rate of transitions between the two states of these centers should have a dispersive character.

Based on the principles and assumptions, and letting

$$N_T = N_L + N \tag{4.1}$$

Redfield and Bube has proposed a rate equation for N(t):

$$\frac{dN}{dt} = \left(\frac{t}{P}\right)^{-\alpha} [C_1 R N_L - C_2 R N + \nu_1 N_L - \nu_2 N] \tag{4.2}$$

where, R is the rate of carrier recombination, which is thought to supply the driving energy for transitions induced by light; C_1 and C_2 are the effectiveness coefficients (i.e., three dimensional cross-sections) for those transitions; ν_1 and ν_2 are effective coefficients of thermally induced transitions; α is the paramater representing the phenomenological dispersive character ($\alpha<1$); and P is the scaling factor that is introduced to preserve the dimensions of all the other coefficients.

Eliminating N_L from Eq.(4.2) by the use of Eq.(4.1) we have

$$\frac{dN}{dt} = \left(\frac{t}{P}\right)^{-\alpha} [N_T(C_1 R + \nu_1) - N(C_1 R + C_2 R + \nu_1 + \nu_2)] \tag{4.3}$$

The rate equations thus appears as

$$\frac{dN}{dt} = \left(\frac{t}{P}\right)^{-\alpha} [G - DN] \qquad (4.4)$$

$$G = N_T (C_1 R + \nu_1) \qquad (4.5)$$

$$D = (C_1 + C_2) R + \nu_1 + \nu_2 \qquad (4.6)$$

where, Eq.(4.5) represents defect generation, and has both light-induced (C_1R) and thermal (ν_1) contributions. Eq.(4.6) represents decay, and has contributions from all the coefficients in the rate equation.

The solution to Eq.(4.3) is a stretched exponential,

$$N(t) = N_s - (N_s - N_0) \exp\left[-\left(\frac{t}{\tau}\right)^{\beta}\right]$$

where $\beta = 1-\alpha$, $N_0 = N(t=0)$ and $\tau^{\beta} = P^{\beta}[\beta/DP]$

$$N_s \equiv \frac{N_T [C_1 R + \nu_1]}{[(C_1 + C_2) R + \nu_1 + \nu_2]} = \frac{G}{D} \qquad (4.7)$$

Here N_0 is the initial defect density and N_S is the steady state value.

In this model, the intermediate value of defect density N(t) thus explicitly depends on the saturation value N_S which depends either on the total number of convertible sites or the balance between light-induced generation and thermal and light-induced annealing.

4.3. Experimental Details

In order to understand the influence of light-induced degradation on the performance of a-Si:H solar cells light-soaking tests were done on two types of structures, namely, pin and pinpin structures. The solar cells used in the degradation experiments were prepared by plasma enhanced chemical vapour deposition (PECVD) technique in a commercial 3-chamber PECVD system on a 10x10 cm^2 substrate. The single junction and the stacked cells have the structures glass/SnO_2/p(C)/buffer/i/n/Ag and glass/SnO_2/p(C)/buffer/i/n/p/i/n/Ag respectively. The area of the cells used in the light soaking experiments is 1x1 cm^2.

The influence of light exposure on the performance of a-Si:H solar cells is investigated using low intensity (~AM1.5) and high intensity (~10AM1.5) illuminations obtained from a WACOM solar simulator. The description of the solar simulator and other apparatus used in the degradation experiments is given in the next section.

All light soaking tests were done under open circuit conditions. Before and after every time interval of light exposure the I-V characteristics of the cells are measured under standard test conditions, i.e., AM1.5 and 25^oC

4.3.1. System Description

In this section a brief description of basic components used in the degradation experiments is given. Some of the equipments used are:

(1) WACOM Solar Simulator and a Fresnel Lens

The increasing efforts to improve the stability of a-Si based solar cells have initiated a means of simulating natural sunlight to perform indoor light soaking tests instead of outdoor, which is climate dependent and a time consuming process. Moreover, the scaling law found between the light intensity (I) and the exposure time (t), i.e., $I^{1.8}t=Constant^{23}$, for the light-induced degradation of a-Si based single junction solar cells, triggered some investigations into accelerated degradation tests which use high intensity illumination. This method helps to evaluate the long-term light induced degradation behaviour of solar cells in a very short time so that a feed back to a deposition laboratory is provided and efforts be made in producing better cells with high stabilized efficiency. Thus, in our degradation experiments, a WACOM solar simulator together with a Fresnel lens was used to perform indoor light soaking tests by low intensity (AM1.5) and high intensity (10AM1.5) illuminations. The schematic diagram of the solar simulator used in the experiment is shown in Fig.4.2.

The WACOM solar simulator consists of xenon short arc lamp (made by WACOM) and halogen lamp (made by KONDO-SYLVANIA) as light sources together with certain optical parts like mirrors, beam splitter and a lens. A mixture of lights from the sources is reflected, transmitted and collimated by the

mirrors and the lens in the solar simulator. The spectrum of the light emerging out of the simulator is in good agreement with the spectral irradiance distribution air mass (AM)1.5 of a natural sunlight as it follows from Fig.4.3 which shows the spectral irradiance distribution of AM1.5 solar radiation and a light beam from WACOM solar simulator.

The light beam from xenon arc lamp gives a radiation in the short wavelength range of AM1.5 while the light beam generated by the halogen lamp has a spectral distribution in the long wavelength range of AM1.5. As is seen in Fig4.3, the spectral irradiance distribution of a simulated solar radiation has little diviation from the reference solar spectral irradiance distribution AM1.5. However, the total irradiance (integrated over all wavelengths) of the simulated radiation is the same as that of AM1.5(100mW/cm^2).

The simulated AM1.5 solar radiation is finally collimated by an output lens of the solar simulator and an area of 140mmx140mm is irradiated. For high intensity illumination, on the other hand, the light emerging out of the solar simulator is further focussed by the use of another lens, namely, Fresnel lens (see Fig.4.5) to an area of slightly greater than the size of a sample solar cell(~1cm^2). The intensity of a light beam falling on the sample during an accelerated degradation experiment can be controlled by changing the position of the Fresnel lens up and down with respect to the sample position. The position of the Fresnel lens is, therefore, fixed at one point above the cell so that high intensity illumination (~10 Suns) is achieved.

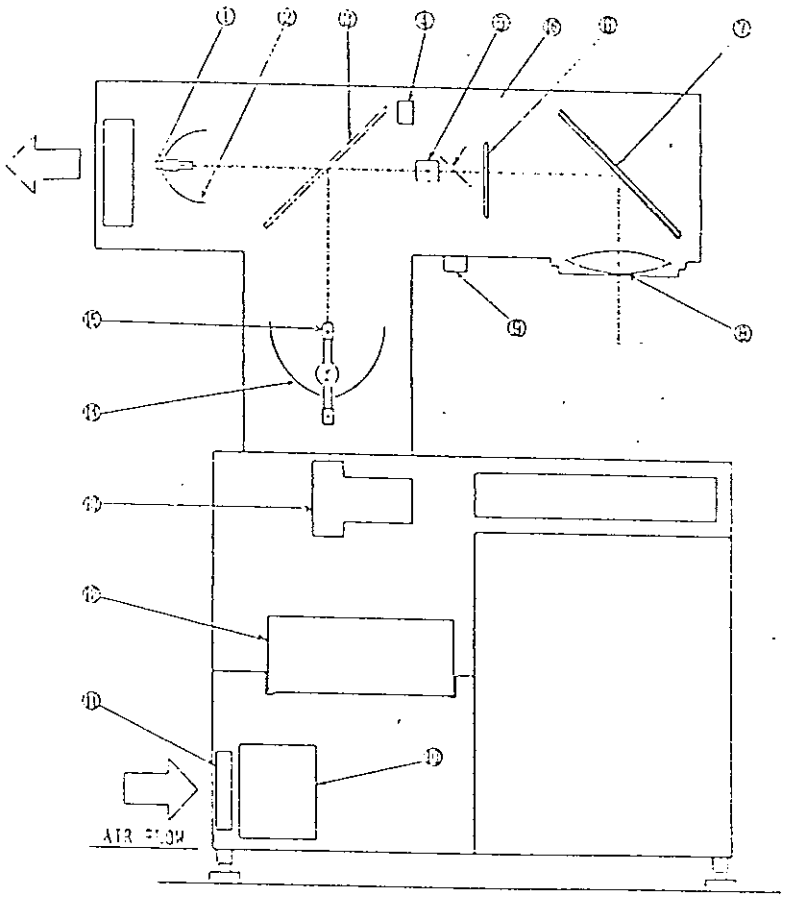

① Halogen Lamp
② Ellipsoidal Reflector
③ Half Mirror
④ Cooling Fan
⑤ Integrator
⑥ Shutter
⑦ Plane Mirror
⑧ Collimation Lens
⑨ Ha. Lamp Feed Back Circuit
Xe. Lamp Feed Back Circuit
⑩ Air Suction Fan
⑪ Pre-Filter
⑫ Hepa Filter
⑬ Cooling Blower
⑭ Ellipsoidal Reflector
⑮ Xenon Lamp
⑯ Beam Splitter

Fig.4.2 A schematic diagram of WACOM solar simulator.

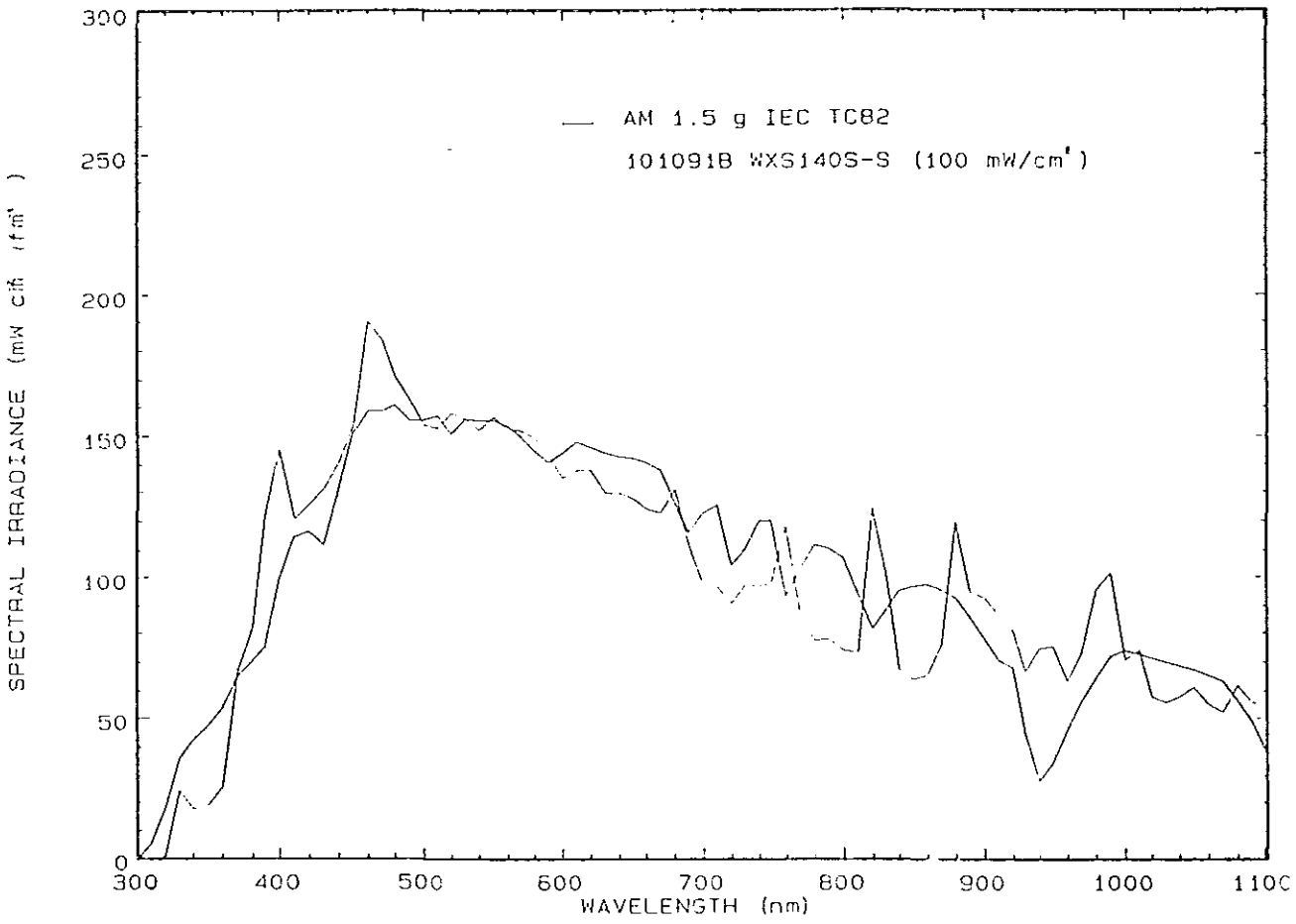

Fig.4.3. The spectral irradiance distribution of AM1.5 solar radiation and a light beam from WACOM solar simulator.

(2) Substrate

The devices which are prepared by 3-chamber PECVD system are deposited on 10x10 cm^2 glass substrate that is coated by SnO_2. The back contact is provided by thermally evaporated Ag. There are 36 solar cells deposited on 10x10cm^2 substrate (Fig.4.4). Most of them have an area of 1 cm^2.

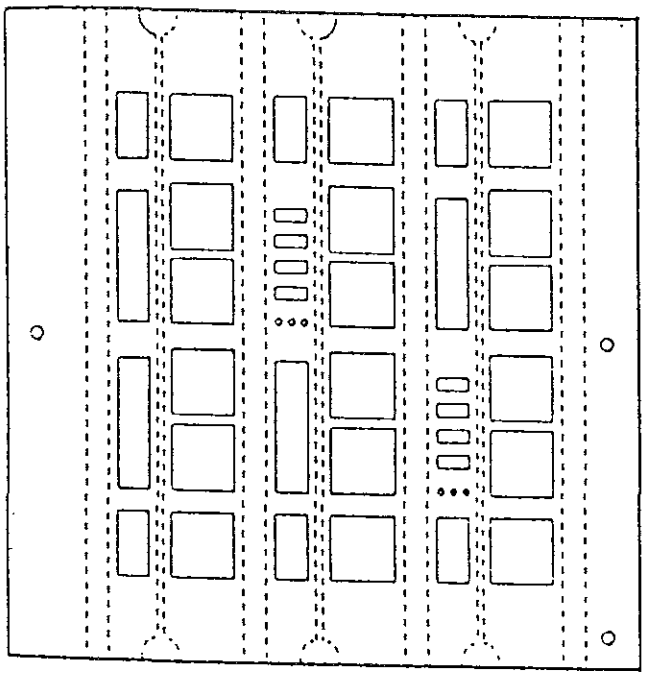

Fig.4.4. A schematic diagram of 10cm*10cm substrate with 36 solar cells.

(3) Gas and Liquid Nitrogen

In order to cool a sample which is under I-V measurement or high intensity or low intensity light soaking tests, a very cold nitrogen gas is blown either upon the sample cell under investigation from above (as shown in Fig.4.5) or upon the whole substrate from the back side. In the experiment, the gas nitrogen is made to flow through a tube which is immersed into a liquid nitrogen (LN_2) where heat exchange between the two

phases takes place. The nitrogen gas then becomes very cold and is blown upon the sample cell or onto the whole substrate.

(4) Temperature control ISI/PV 9007H;pt 100

These are devices used for measuring the temperature of a sample solar cell, or controlling its value about a certain degree centigrade. For instance, the temperature of a cell, according to the standard test condition, must be kept at $25^{o}c$ during light/dark I-V measurement. Also, during light exposure the temperature of the sample is usually maintained at a particular value (say $50^{o}c$). Thus, the above devices allow to keep the temperature of the cell with an accuracy of approximately $\pm 1^{o}c$.

(5) Low Voltage Power Supply NTN 350-20

In an effort to cool the solar cell during the degradation experiment big temperature gradient can be created with in the glass substrate between the irradiated cell and its surroundings. The temperature gradients create tension within the substrate between the two regions and, obviously, bring mechanical damage to the sample cell or other parts of the substrate. Thus, to minimize this temperature gradient, the surrounding of the cell is sometimes heated by a nitrogen gas which is made to pass through a resistor (shown as heater in Fig.4.5) connected to the low voltage power supply NTN350-20. This power supply allows some current (I) to pass through the resistor (R) thereby producing heating power I^2R. The heat produced is drawn by a nitrogen gas which is directed to the substrate. Sometimes this arrangement, controlled by temperature control 9007H, also uses to heat the sample itself to some higher temperatures.

In general, the temperature of a sample can be lowered or raised using nitrogen gas flow which can be cooled or heated by liquid nitrogen (LN_2, in Fig.4.5) or the resistor (heater), respectively.

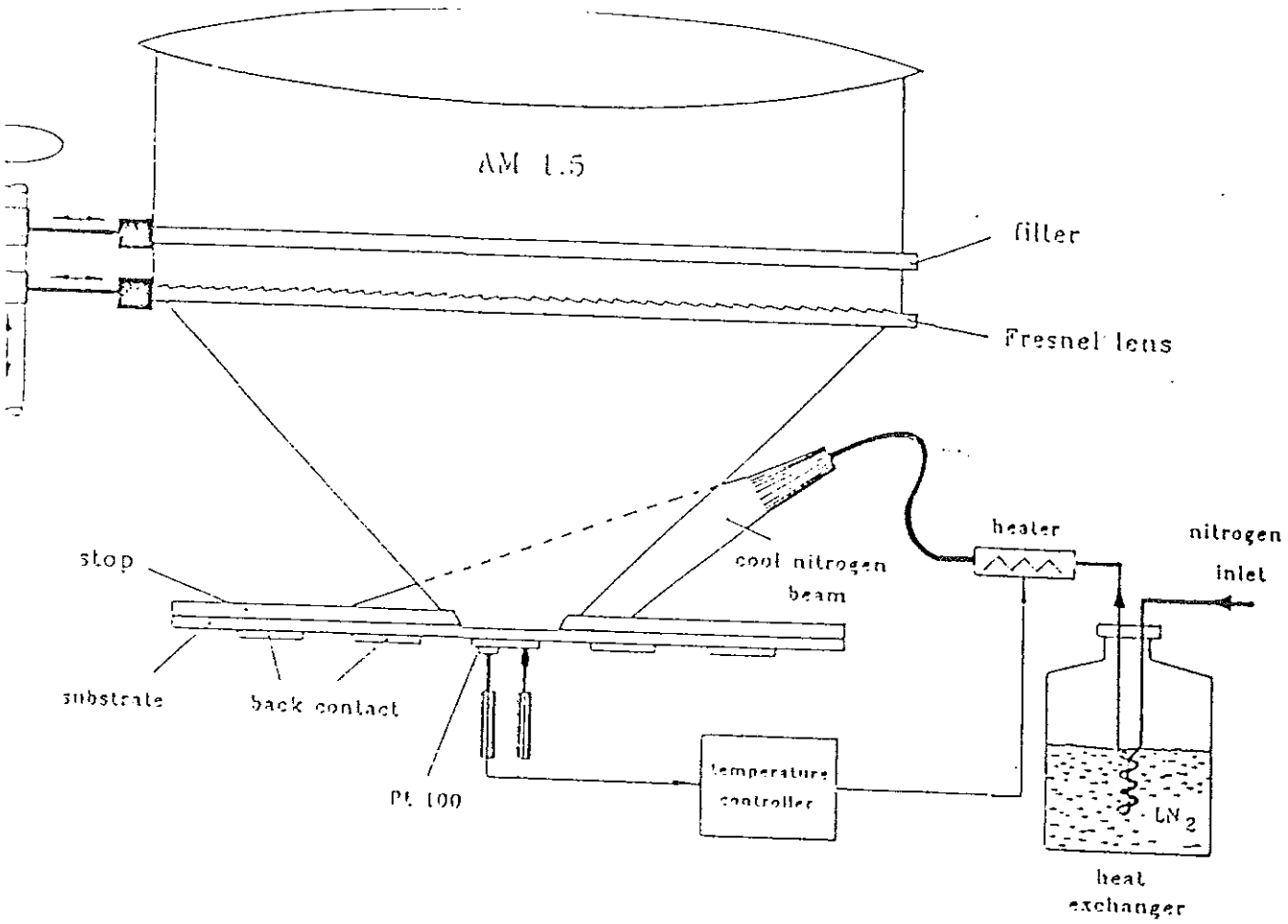

Fig.4.5. A schematic diagram for the arrangement of some apparatuses used during light exposure.

(5) High current source measuring unit (SMU); computer

The SMU, controlled by a key board entry at a PC connected with the degradation experiment apparatus, is used to measure the light and dark I-V characteristics of a solar cell by sweeping an applied voltage to the cell.

4.3.2. Experimental procedure

The following procedures have been followed to perform the light-induced degradation experiment which may be divided into two parts:

(1) I-V measurement

1.1. The solar simulator is turned on and the shutter is opened from the mains.

1.2. The primary task before starting any measurement is the test on the homogeneity of the irradiation from the solar simulator. Thus, the homogeneity of the radiation is first tested over a certain area (approximately the size of a substrate, i.e.,10cmx10cm) using a particular reference cell to some standard irradiance of the simulated radiation which produces a current of ~ 10.52mA/cm^2. The uniformity of this value is checked over ~10cmx10cm region by moving the reference cell around a number of points (nine points to be exact) at the position of the substrate and measuring the current produced due to the simulated irradiation at these points. For a good working condition, therefore, the

deviation in homogeneity of the illumination over the whole area must not exceed $\pm$2%.

A large deviation from the average value (~10.52mA/cm^2) can be corrected by adjusting the mirrors in the solar simulator. Inorder to identify which one of the lamps is responsible for the deviation one may use filters that absorb long wavelength or short wavelength radiations and then compare the value of irradiance with the corresponding standard value of irradiance from the tungsten lamp or xenon lamp.

1.3. The substrate is mounted on a temperature controlled stage facing the emerging radiation from the smulator, which consists a number of pins that make back contact with the cells on the substrate. The contact between the cells and the pins is controlled by electric relays which are switched on/off using a key board entry. The command at the pc makes a pin to be intouch with a cell under investigation and thus the SMU and the cell form a closed circuit.

1.4. While shielding the cell from light, the dark I-V characteristics is measured by sweeping the voltage from -1V to 1V using SMU and a key board entry at PC.

1.5. The cell is then illuminated and light I-V characteristics is measured as voltage is swept (from -0.2V to 1V) as in procedure 1.4.

(2) Light soaking test

We did our degradation experiment under open circuit condition using high intensity (~10 Suns) and low intensity (~1 Sun) illuminations. Thus, let us divide again this part into two parts:

2.1. Low intensity light soaking.

2.1.1. The cell under investigation is simply illuminated by a radiation coming from the solar simulator (~AM1.5) while the rest cells on the substrate are protected from light by a mask or stop which has an opening a little larger than the dimension of a cell (1cm*1cm).For a light soaking test under open circuit condition the sample cell should not make back contact with a pin behind it during illumination so that the circuit becomes open.

2.1.2. After every time interval (say 1s, 10s, 100s, 1h, etc.) the dark and light I-V measurements are done according to procedure (1.4) and (1.5).

2.2. High intensity light soaking test.

2.2.1. A Fresnel lens intercepts the light emerging out of the solar simulator (Fig.4.4).The position of the lens is adjusted in such a way that the converged light beam which emerges out of the lens is fully incident on the sample cell and homogeneity is optimized.

2.2.2. The cell is then illuminated by high intensity (~10 Suns) light beam which appears from the Fresnel lens while the rest cells are protected in the same manner as in low intensity degradation experiment (procedure 2.1.1.). Also, the cell and the pin are not in touch with each other for the experiment is done under open circuit condition.

2.2.3. Dark and light I-V measurements are done after every time interval according to procedure (1.4) and (1.5).

4.3.3. Experimntal Results and Discussion.

In order to understand the light-induced degradation behavior of a-Si:H solar cells a number of light soaking tests were performed on pin and pinpin structures under high intensity and low intensity illuminations. The light soakings were done under open circuit conditions. During all light exposure tests (except in one experiment) the temperature of the cells under investigation was kept at 50^{o}c. On the other hand, the photovoltaic characteristics, i.e. V_{oc},J_{sc},FF and η of the cells were measure under standard test conditions (AM1.5, 25^{o}c).

Some of the questions that we tried to understand from the experiments are:

PIN STRUCTURE

- What is the pattern of degradation of pin junction solar cells?
- Comparison of high intensity and low intensity

degradation experiments?
- What is the effect of temperature on the degradation of a-Si:H pin solar cells?
- Can saturation be reached by pin junction solar cells under high intensity illuminations at 50°c.

PINPIN STRUCTURE

- Comparison on the stability of pin and pinpin structures.
- Thickness dependence of light induced degradations in pinpin structure solar cells.
- Comparison between high intensity and low intensity light soaking tests on pinpin structures.
- What is the pattern of degradation of stacked cells.
- Can saturation be reached by tandem solar cell under high intensity illuminations at 50°c.

PIN STURCTURE

1) The pattern of degradation of pin junction solar cells:

The first question that arises in an effort to understand the degaradation behavior of a-Si:H pin junction solar cells is: what is the degradation pattern of a pin junction solar cell, i.e., which parameter of V_{OC}, I_{SC} and FF degrades faster and which one of them degrades less? In other words, which parameter(s) cause the degradation in efficiency of a-Si:H pin solar cells? To answer this question we did light soaking tests both under high intensity (~10AM1.5) and low intensity (~AM1.5) illuminations under open circuit condition at 50°c. The results are shown in Fig.4.6(a) and Fig.4.6(b).

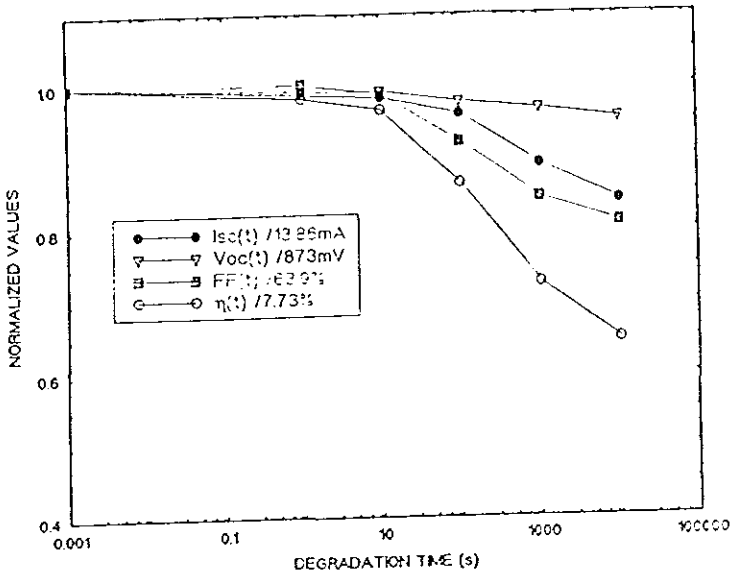

(a)

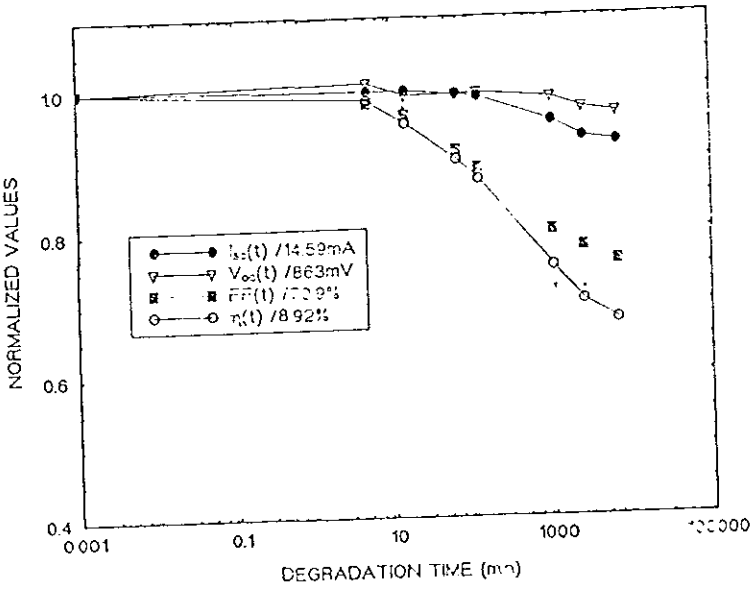

(b)

Fig .4.6 Light-induced degradation of a-Si:H pin solar cell parameters under 10 suns (a), and under 1 sun (b) at 50°c and open circuit conditions.All values are normalized to initial ones.

As is evident from the two figures, the degradation in efficiency comes mainly from fill factor and partly from short-circuit current in both the high intensity and low

intensity light soaking tests. For our samples the degradation in open circuit voltage V_{OC} is very small. This result is in agreement with the experimental result of some researchers[24,25] who believe that the degradation of cell performance is mainly attributed to the decrease of carrier collection due to the light-induced creation of metastable defects in the intrinsic layer, which act as recombination centers. This reduces the fill factor and short-circuit current while the open circuit voltage is only slightly affected.

(2) Comparison of high intensity and low intensity degradation experiments:

There is a scaling law between the light intensity (I) and the exposure time (t), i.e., $I^{1.8}t=$constant, proposed by A. Catalano et.al.[23] for the light-intensity dependence of cell degradation of single junction a-Si:H solar cells. This law provides a useful tool to determine the degradation behavior of single junction solar cells through the use of accelerated degradation test. We have, therefore, made light soaking tests to check if the law holds for our samples too. Thus, we did high intensity (10 Suns) and low intensity (1 Sun) light exposure experiments under open circuit conditions on sample cells which are prepared during the same process on the same substrate. The cell temperature was maintained at 50^{o}c during light soaking. plotted in Fig.4.7 are the degradation curves of normalized efficiencies versus exposure time on a logarithmic scale for the two light intensities. Also, in the figure, the degradation curve of normalized efficiency under 10 Suns is rescaled according to the scaling law so as to compare it with the degradation curve of normalized efficiency under low intensity.

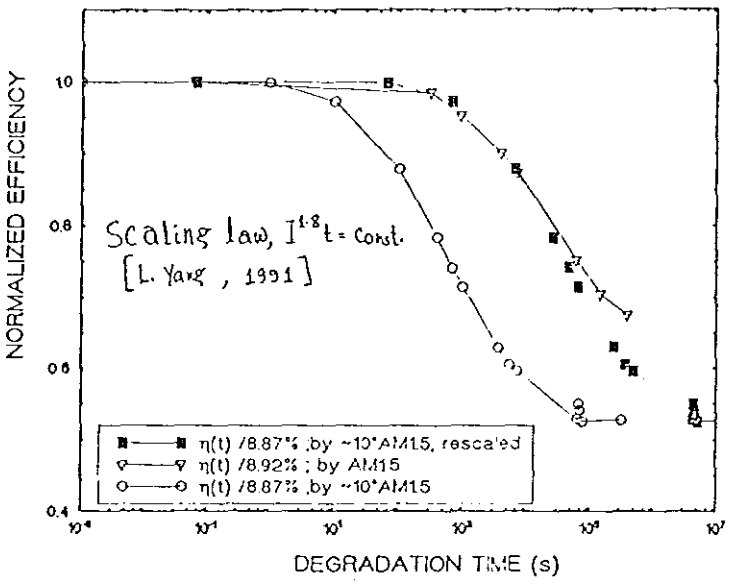

Fig.4.7: Normalized cell efficiency versus light exposure time at AM1.5 and 10 AM1.5 illuminations. The temperature was maintained at 50°c during light exposure.

As shown in the figure, the degradation behavior of the single junction solar cell under high intensity illumination fits over a wide range of time with that of low intensity illumination when rescaled using the scaling law. Thus we may conclude from our result that the scaling law $I^{1.8}t$=const, proposed by A.Catalano et.al., holds for our samples too. Therefore, the outdoor degradation behavior of our single junction samples can be predicted from an indoor accelerated test in a very short time.

(3) The effect of temperature during degradation

The effect of temperature on the stability of a-Si:H pin junction solar cells was studied by making high intensity light soaking tests under open circuit condition at 28°c and 50°c. The cells under investigations were prepared under the same deposition conditions. After 10,000s light exposure, it is found that (Fig.4.8) the degradation in efficiency of a cell at 50°c is relatively smaller than that of a cell at 28°c. From our experimental result we conclude that the degradation in efficiency of a-Si:H pin solar cells depends on the temperature of the cell during light soaking. This is, therefore , an indication that there exist competing effects,

i.e., light induced defect generation and thermal and light induced annealing even for temperatures as low as 50°c during light soaking .

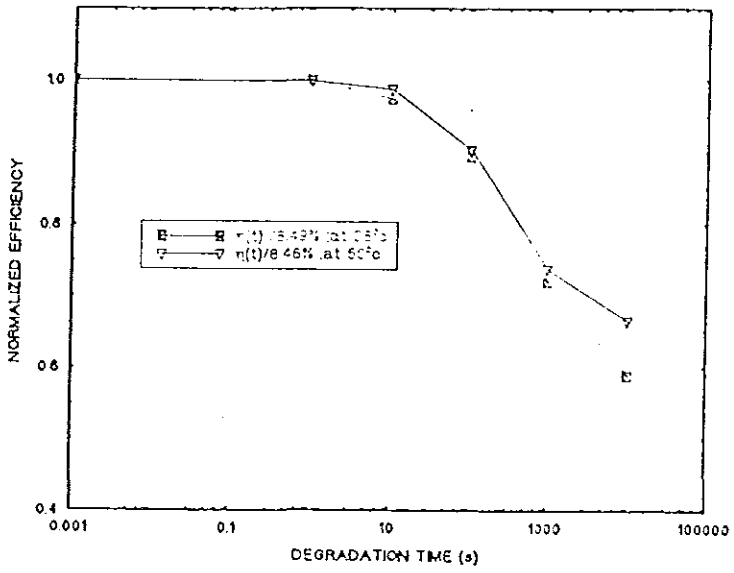

Fig 4.8 Light-induced degradation of a-Si:H pin solar cells at 28°c and 50°c under 10 Suns illumination.

(4) Saturation of Light Induced Degradation

As mentioned repeatedly the main source of degradation present in a-Si:H solar cells is associated with the creation of metastable defects in a photovoltaic active region. The simplest model for the drop in cell efficiency during operation ties the cell efficiency to the fill factor, the fill factor to the collection length, and the collection length to the defect density N(t)[26].As is shown in the

stretched exponential model of Redfield and Bube the defect density N(t) is linked to the saturation value N_S. Even though, there have been disagreements on the origin of defect generations as well as the mechanism for defect saturation, there is no question that the metastable defect saturate at some value.

In general two mechanisms can explain saturation of defects quantitatively. One straight forward explanation is the depletion of precursor sites that can be converted to defects. Another mechanism for defect saturation is a steady state balance between light induced generation and thermal and light induced annealing. Based on these different models a number of questions remained unanswered regarding the stability of a-Si:H solar cells at higher efficiencies. One of the questions that remained to be answered is whether the light induced degradation will reach saturation at low temperatures. Thus, we have made a degradation experiment on our single junction sample to see if saturation of solar cell parameters could be achieved when the cell is exposed to high intensity illumination (10 Suns) at 50^{o}c. We did the experiment under open circuit condition.

While there is no evidence from our measurements that saturation occurs due to the exhaustion of all convertible defect sites or the balance between light induced degradation and thermal and light induced annealing, it did occur at 50^{o}c under high intensity (10 Suns) illumination. Of course, this result is in contrast to the result of L.Yang et.al.[27] who claim that saturation was not observed at 50^{o}c after an equivalent one sun exposure time of over 25000h. In our experiment (see Fig.4.9) saturation was observed afetr 1386 hr of AMI.5 equivalent light soaking at 50^{o}c.

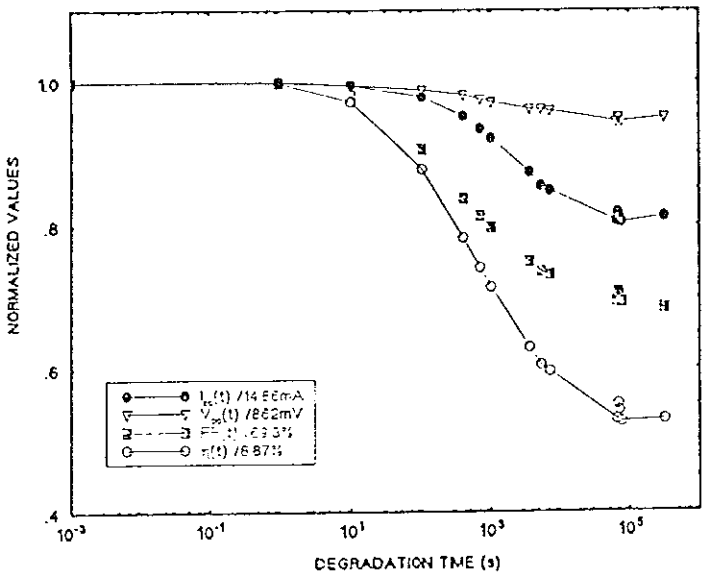

Fig.4.9. Saturation of light-induce degradation of a-Si:H pin solar cells. During light exposure the temperature was maintained at 50°c. The light soaking was done under open circuit condition.

PINPIN STRUCTURE

(1) Comparison on the stablity of pin and pinpin structure solar cells under hight intensity illuminations.

The most important problem in the field of solar cells is to obtain high conversion efficiency and stable operation under sunlight. During the past decade, it has been recognized that the preparation of stacked, multijunction cells may provide a solution to the light instability problems of amorphous silicon based solar cells. Thus, we have made light soaking tests on our pinpin structure samples to see if stability of a-Si:H solar cells is improved by using this structure. Fig.4.10(a) shows the comparison between pin and pinpin structure solar cells under high intensity (10 Suns) illumination. The comparison shows that even the most

degrading type of our stacked sample exhibit a better stability than a single junction solar cell.

We have also made another set of light exposure tests to compare the light-induced degradation of single junction and tandem structures under low intensity (1 Sun) illumination. As is seen in Fig.4.10(b), our stacked samples still show better stability than pin structure solar cell.

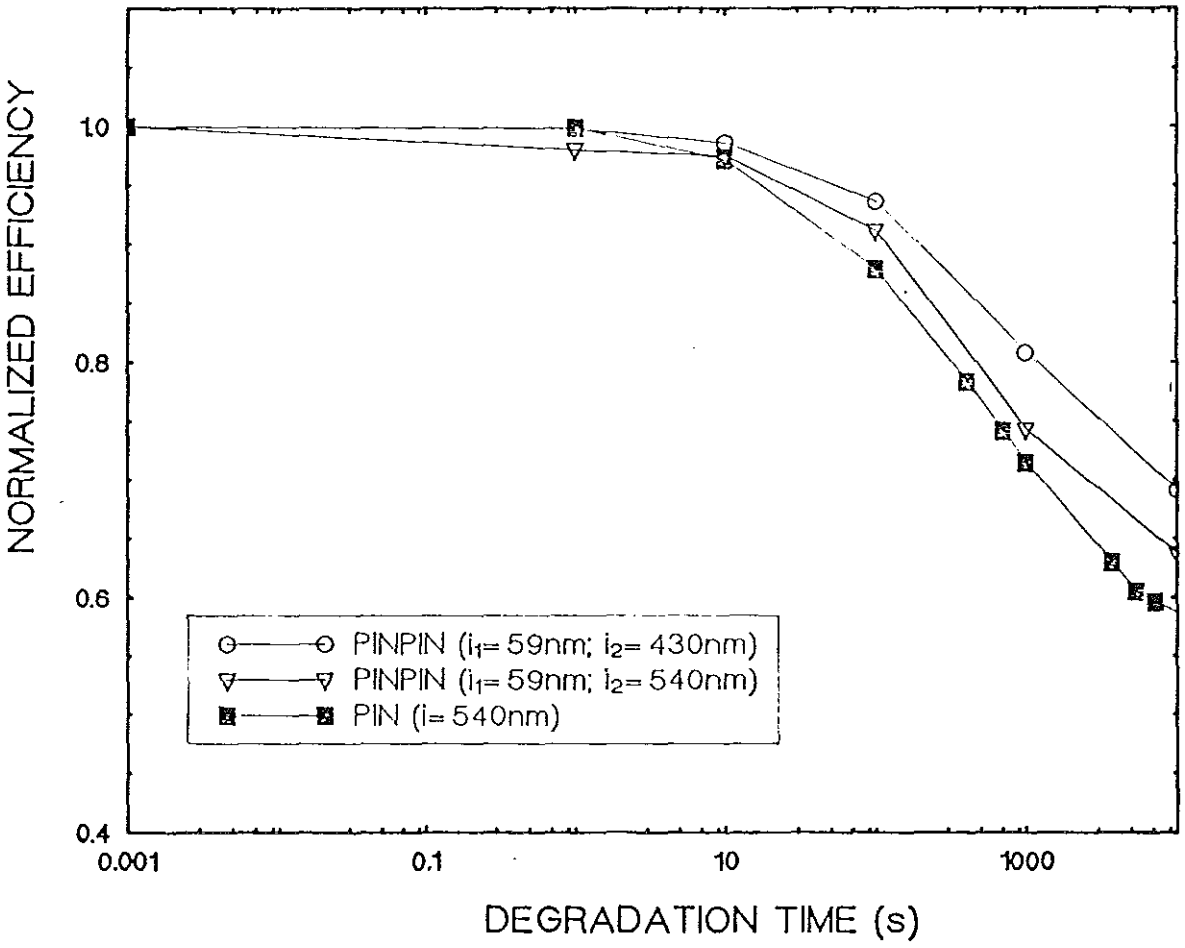

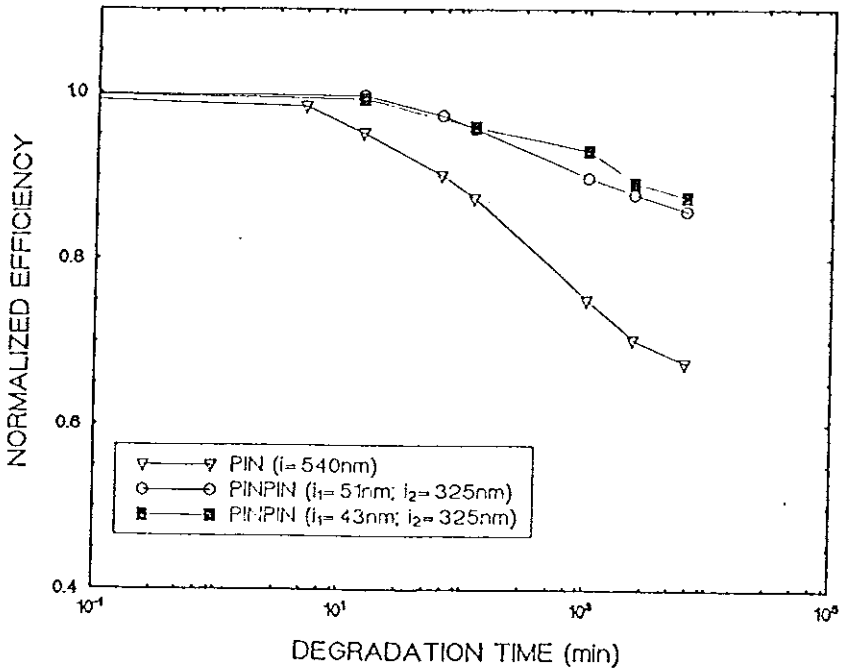

Fig.4.10. Degradation in efficiency of pin and pinpin a-Si:H solar cells. The light soaking was done under 10 Suns(a) and 1 Sun (b) at 50^{o}c and open circuit condition.

(2) Thickness dependence of light-induced degradations in pinpin structure solar cells.

The thickness dependence of light induced degradations of a-Si:H pin junction solar cells has been studied by a number of groups. It has been found that the stability of a-Si:H single junction solar cells can be greatly improved by reducing the thickness of the i-layer[28].Thiseffect is commonly attributed to the larger electric field present in the thin cell which sweeps carriers across the device more easily

making it less sensitive to light induced defects in the i-layer[29]. On the other hand, for pinpin structure of a-Si:H solar cells this observation has not been demonstrated experimentally . Logically, one would expect to obtain a similar thickness dependence as in the case of a single junction solar cells. To prove this we performed light soaking tests on different i-layer thicknesses, where i-layer thickness of the stacked cell is the sum of the i-layer thicknesses of the top and bottom cells, under 10 Suns and 1 Sun illuminations.

It can be seen from Fig.4.11 that the light-induced degradation is suppressed as the i-layer thickness is reduced. After 10^4s the highest decrease in efficiency was obtained for a cell with maximum i_1 and i_2. The effect of i-layer thicknesses on the decay in efficiency of pinpin solar cells is clearly manifested under high intensity illuminations even for the slight difference of the top layer thicknesses (See normalized efficiency versus exposure time curves for cells with i_1=43nm; i_2=325nm and i_1=51nm; i_2=325nm, Fig.4.11). However, the light soaking tests under low intensity illumination (Fig.4.12) made on cells with top layer thickness i_1 of 43nm and 51nm (i_2=325nm) did not result such a big difference on the stability as high intensity light soaking tests. Of course, the cell with smaller i-layer thickness is at a better stability for the entire time of light exposure as is expected. This effect may be attributed (as will be described shortly) to the strong loss in efficiency of stacked cells under high intensity (10 Suns) light soaking tests than under low intensity (1 Sun).

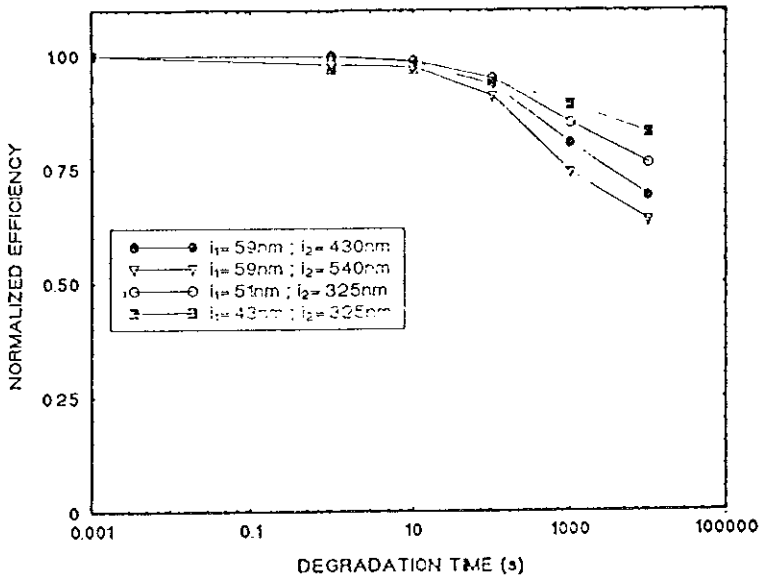

Fig.4.11. Normalized efficiency of stacked cells with different i_1- and i_2-layer thicnesses as a function of the illumination time under 10 Suns (10 AM1.5, 50°c).

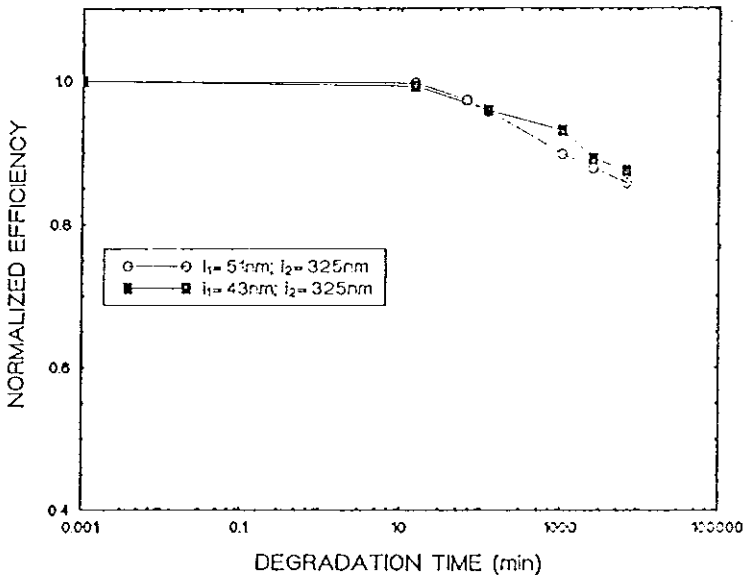

Fig.4.12. Normalized efficiency of two stacked cells with different i_1- and i_2-layer thicknesses as a function of the illumination time under 1 Sun (AM1.5, 50°c).

(3) Comparison between high intensity and low intensity light

soaking tests on pinpin structure:

In a single junction a-Si:H solar cell the light-induced degradation behavior of the cell under low intensity illumination can be predicted from accelerated light soaking tests using the scaling law ($1^{I \cdot 8}t$=Constant). How about in stacked cells? Does the scaling law hold for pinpin structures as well? To answer these questions we performed light soaking tests under low intensity and high intensity illuminations and compared the light induced degradation behavior of stacked cells under high intensity and low intensity illuminations.

In Fig.4.13 we compare the degradation of two stacked cells under 1 Sun and 10 Suns. The cells were prepared during the same process on the same substrate. The time axis of the high illumination experiment is rescaled by the scaling law. The efficiency shows a significantly smaller degradation under 1 Sun (14% of the initial value after 1000h) than under high intensity illumination (24% of the initial value after a time corresponding to 100h).

Though, it is difficult to draw any conclusion at this stage, our result gives a clue that the scaling law may not hold for stacked cells and should be modified. Accelerated degradation tests can be used to compare the decay in absolute efficiencies among different stacked cells which are prepared under various deposition conditions so that feed back may be offered to deposition laboratories in short time. However, care should be taken when deducing the light induced degradation behavior of stacked cells under low intensity (AM1.5) illumination from accelerated tests using the scaling law.

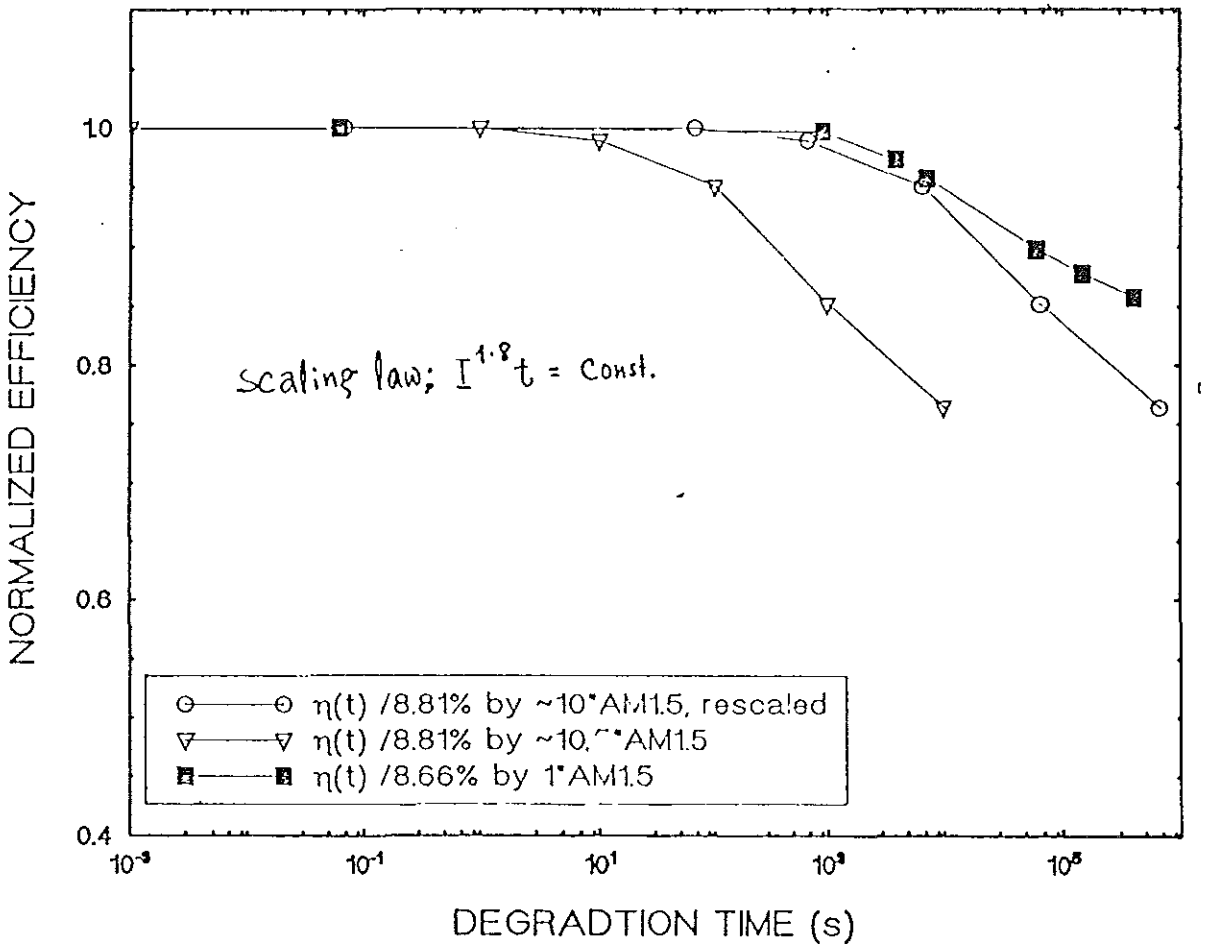

Fig.4.12. Normalized efficiency of two similar stacked cells (i_1=51nm and i_2=325nm for both cells) as function of the illumination time for the 1 sun experiment (AM1.5, 50°c) and the rescaled illumination time for the 10 Suns experiment (10.AM1.5, 50°c).

4. The pattern of light-induced degradation of pinpin structure solar cells.

In all our single junction samples we observe a uniform degradation patter during light soaking tests, i.e., the degradation in efficiency mainly comes from fill factor and partly from short circuit current while open circuit voltage being the less affected parameter (see Fig.4.6(a) and (b)). However, in pinpin structure solar cells, we do not observe such uniform degradation pattern as it is evident from Fig.4.14. Of course, similar to the pin structure, the degradation in efficiency of all stacked cells mainly comes from fill factor. But the decrease in short circuit of stacked cells under illumination depends on the type of the cell under consideration. In some stacked cells (Fig.4.14(a) and Fig.4.14(b)) the degradation in short-circuit current (I_{SC}) is very small, almost negligible, while in others (Fig.4.14(c) and Fig.4.14(d) the degradation in $I_{SC}$is quite significant as in the case of single junction solar cells.

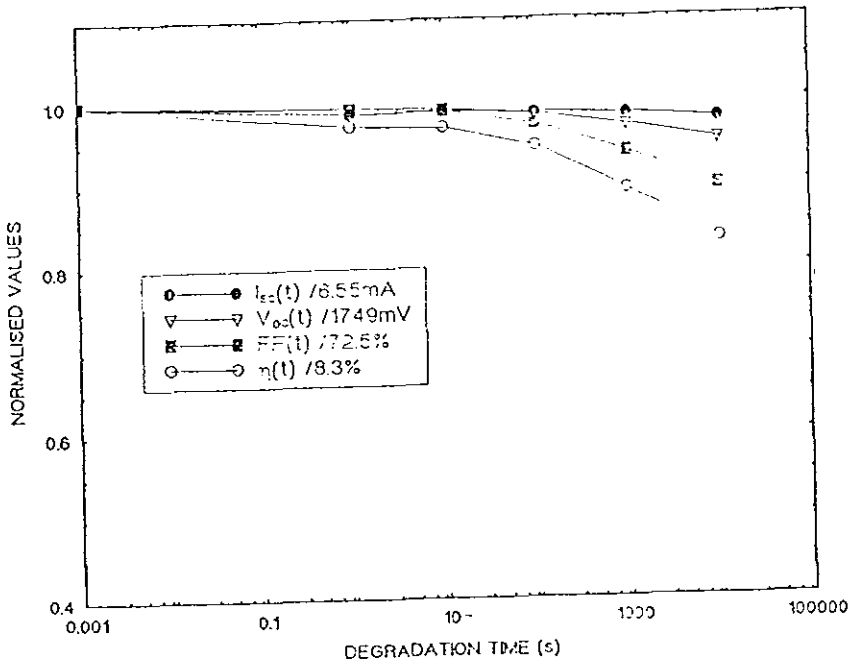

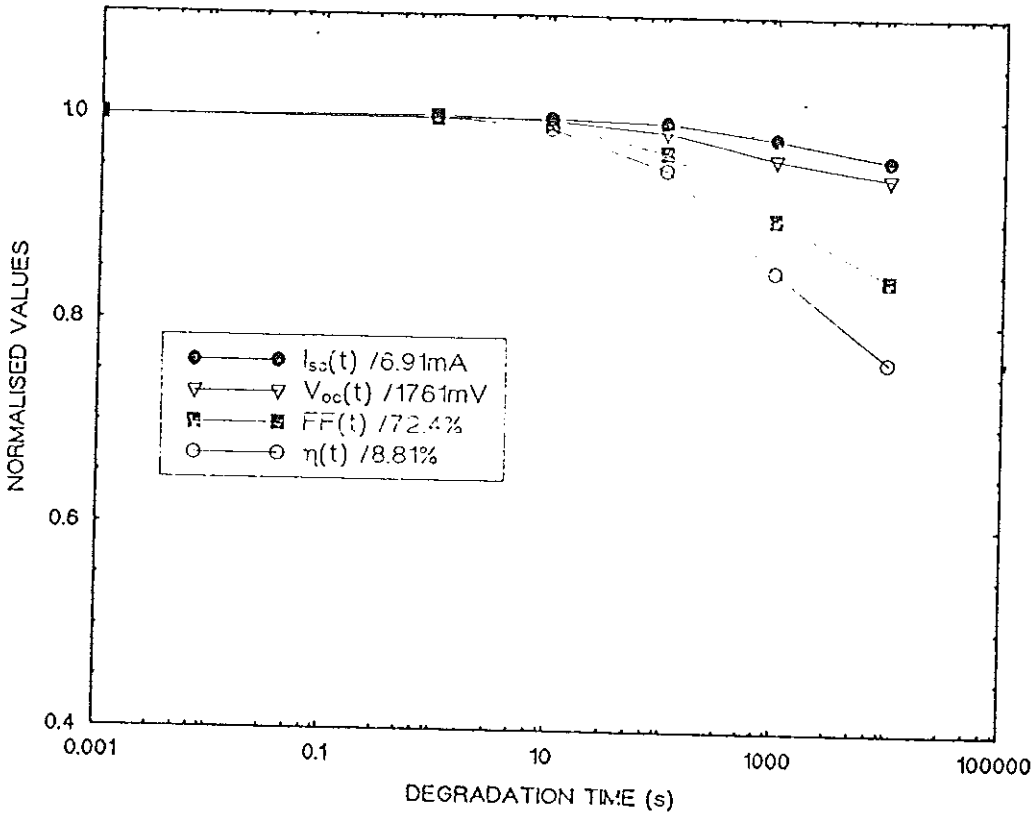
NORMALISED VALUES
1.0
0.8
0.6
0.4
0.001
0.1
10
1000
100000
DEGRADATION TIME (s)
I_{sc}(t) /6.91mA
V_{oc}(t) /1761mV
FF(t) /72.4%
η(t) /8.81%

(b)

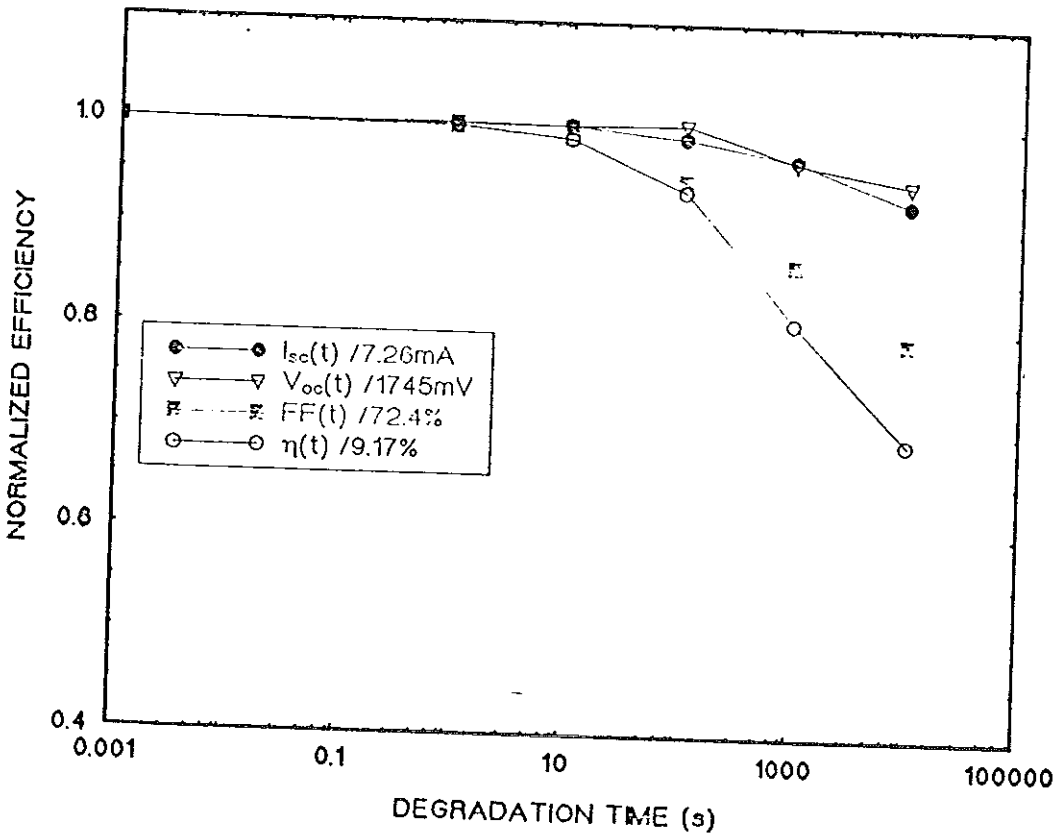
NORMALIZED EFFICIENCY
1.0
0.8
0.6
0.4
0.001
0.1
10
1000
100000
DEGRADATION TIME (s)
I_{sc}(t) /7.26mA
V_{oc}(t) /1745mV
FF(t) /72.4%
η(t) /9.17%

(c)

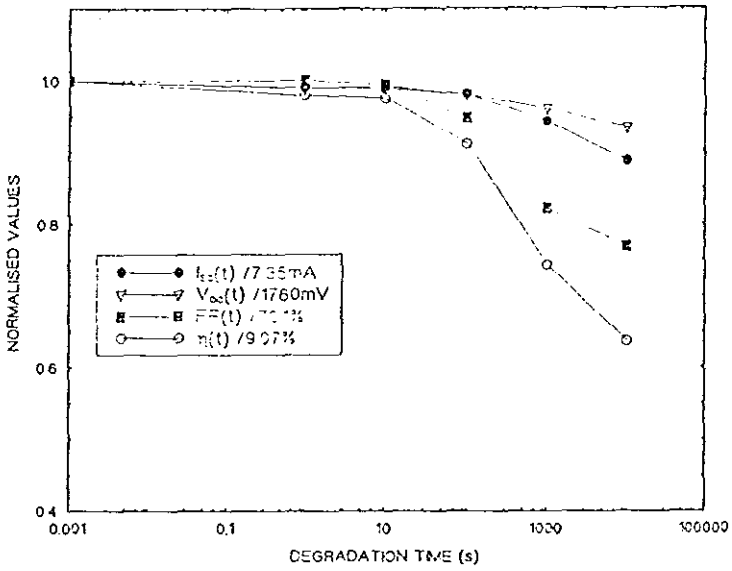

(d)

Fig.4.14. Light induced degradation of a-Si:H pinpin solar cells with different i-layer thicknesses:(a) i_1=43nm; i_2=325nm (b) i_1=51nm; i_2=325nm (c) i_1=59nm;i_2=430nm and (d) i_1=59nm;i_2=540nm. The light exposure test was made under 10 Suns (10 AM1.5) illuminations (50^{o}c and open circuit condtion).

A closer look at the degradation behavior of the stacked cells reveals that those cells with thick bottom layers (Fig.4.14(c) and Fig.4.14(d)) exhibit a degradation pattern similar to that of single junction solar cells, i.e., the degradation in efficiency comes from the fill factor and the short circuit while open circuit voltage being degraded slightly. On the other hand, those cells which have relatively thin bottom layers show a different degradation pattern as shown in Fig.4.14(a) and Fig.4.14(b), i.e., the degradation in short-circuit current is negligibly small. This difference in degradation pattern, specially the difference in the degradation of Isc, may be due to the current limitation of stacked cells.

There is a well established consensus among photovoltaic

specialists[30] that the output current of stacked solar cells is limited by the lowest current among the component cells. Thus, in those stacked cells whose current is limited by the top cell, the degradation in short-circuit current should be negligible since the large electric field present in the top cell (which has a thickness ~60nm) sweeps away the electron-hole pairs created in the layer before they can recombine and create light-induced defects in the layer. However, if the current is limited by the bottom cell, the degradation in I_{sc} as well as the degradation pattern of the stacked cell in general resembles that of single junction solar cells. Thus, we may conclude that the degradation in I_{sc} of stacked cells is limited by that component (top or bottom) of the tandem structure which has smaller output current.

(5) Saturation of light induced degradation of a-Si:H pinpin solar cells:

A number of studies have been made on the stability of light induced degradation of a-Si:H pin junction solar cells. However, little is known on the saturation of light induced-degradation of a-Si:H pinpin solar cells. To understand this issue, we performed light soaking test on a stacked cell under high intensity (10 Suns) illumination at 50°c. As is evident from Fig.4.15, saturation of solar cell parameters did occur in pinpin structure at 50°c under 10 Suns illumination. Moreover, comparison of the level of saturation in pin and pinpin structures (Fig.4.16) shows that the light-induced degradation of a-Si:H solar cell parameters saturate at relatively higher values in pinpin structure than pin structure.

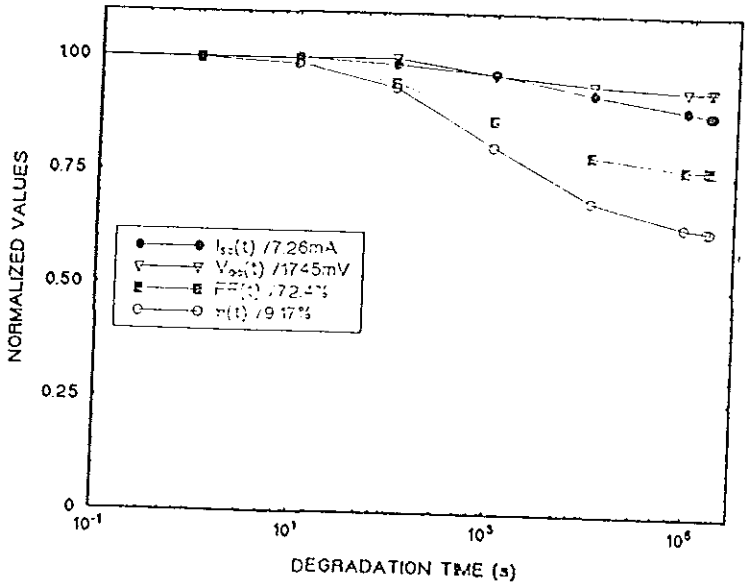

Fig.4.15.Saturation of light-induced degradation of a-Si:H pinpin solar cell parameters. The light exposure test was made under 10 Suns (at 50°c and open circuit condition).

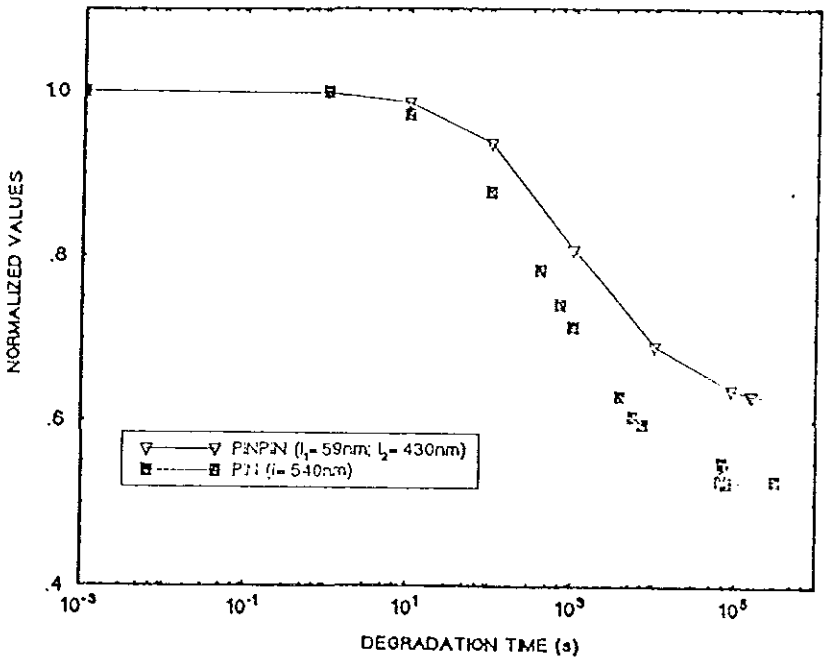

Fig.4.16. Level of saturatiobn of light-induced degradation of pin and pinpin structures. The plot shows the normalized efficiency of both structures as a function of light exposure time.(50°c and 10 AM1.5)

CONCLUSION

PIN STRUCTURE

The degradation in efficiency of a-Si:H single junction solar cells mainly comes from fill factor (FF) and partly from short-circuit current (I_{SC}).Onthe other hand, the degradation in the open-circuit voltage (V_{OC})isvery small in all our samples.

The degradation in efficiency of a-Si:H solar cells depends on the temperature of the cell during light soaking. Those cells at higher temperatures during illumination show better stability than cells at lower temperatures. This may be attributed to the balance between light-induced degradation and thermal and light-induced annealing even for temperatures as low as 50^{o}c during light soaking.

The scaling law between the light intensity (I) and the exposure time (t), i.e., $I^{1.8}t$= constant, proposed by A.Catalano et.al.[23],holdsfor our pin junction samples as well.Thus ,the out door degradation behaviour of our single junction samples can be predicted from an indoor accelerated test in a very short time.

Inspite of the experimental result proposed by some groups (L.Yang et. al.[27])saturation is observed under high intensity illuminations (10 Suns) at 50^{o}c after 1386h of AM1.5 equivalent light soaking.

PINPIN STRUCTURE

Stacked cells are more stable than single junction solar

cells.

The stability of a-Si:H pinpin solar cells depends on the i-layer thickness. Cells with thin i-layer thicknesses show better stability than cells with thick i-layer thicknesses.

Stacked cells show better stability under low intensity light exposure than high intensity. Though accelerated degradation tests can be used to compare the decay in absolute efficiencies among different stacked cells in a very short time, care should be taken in drawing conclusions about the light-induced degradation behaviour of pinpin cells under AM1.5 from high intensity light soaking tests.

The degradation in short circuit current I_{SC} of stacked cells is limited by that component (top or bottom) of the tandem structure which has smaller out put current.

Saturation of solar cell parameters is observed in pinpin structure at 50^{o}c under 10 Suns illumination. Also, the light-induced degradation of a-Si:H solar cell parameters saturate at relatively higher values in pinpin structure than pin structure.

APPENDIX A

Derivation of the Current-Voltage relationship for a P-n junction Diode.

First of all let us derive the expression for built-in voltage V_0 across the transition region of a P-n junction. It can be calculated in the following manner. In thermal equilibrium the conduction-electron current is zero, i.e

$$J_n = 0 = q n_o \mu_n E + q D_n \frac{dn_o}{dx} \qquad (A.1)$$

where n_o is the density of conduction electrons in thermal equilibrium, μ_n is the electron mobility, D_n is electron diffusion coefficient.

Then

$$-E = \frac{D_n}{\mu_n n_o} \frac{dn_o}{dx} \qquad (A.2)$$

but, using the Einstein relations $D_n = \mu_n \frac{KT}{q}$ and the relation between potential and electric field from the electrostatic, we have

$$\frac{dV}{dx} = \frac{KT}{q n_o} \frac{dn_o}{dx} \qquad (A.3)$$

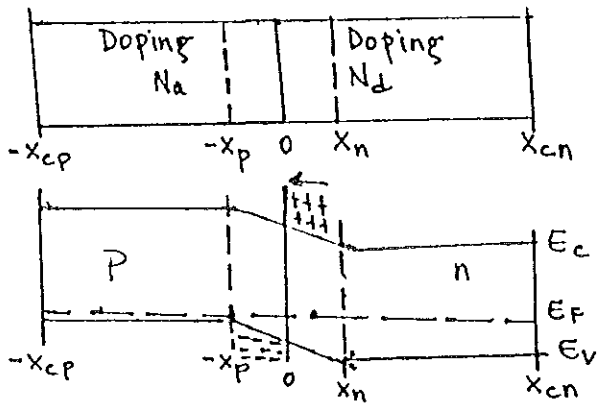

Fig. A.1. The geometry (a) and band diagram (b) for an abrupt 'n junction diode.

ntegrating this from $x = -x_p$ to $x = x_n$ yields

$$V(x_n) - V(-x_p) = KT/q \ln n_o(x_n)/n_o(-x_p) \quad (A.4)$$

Then we define

$$V_o \equiv V(x_n) - V(-x_p) \text{ in equilibrium.}$$

If it is assumed that all impurities are ionized, $n_o(x_n) = N_d$ and $n_o(-x_p) = n_{io}^2/N_a$ (Here N_d and N_a are the concentration of donors and acceptors respectively). Substituting these into Eq.(A.4) results in

$$V_o = KT/q \ln N_d N_a/n_{io}^2 \qquad (A.5)$$

Returning back to Eqn (A.1), under equilibrium conditions the net conduction-electron current density is zero. However the two terms, i.e, the drift term - $qn_{o\mu n}E$ - and the diffusion term - $qD_n\, dn_o/dx$ - are individually very large compared to the current density when there is a slight deviation from the zero bias condition. The zero current is therefore the result of a delicate balance between two large components in opposite directions. It is reasonable to assume that a small bias voltage will disturb this balance only slightly. then we can say that

$$J_n \cong 0 = qn\mu_n E + qD_n\, dn/dx \quad (A.6)$$

Now let us determine the carrier concentration at the edges of the transition region. If it is assumed that all the applied voltage appears across the transition region,

$$V(-x_p) - V(x_n) = KT/q \ln n(-x_p)/n(x_n) \qquad (A.7)$$

but $V(-x_p) - V(x_n) = V_a - V_o$, where V_a is the applied voltage. Thus,

$$V_a = KT/q \ln n(-x_p)/n(x_n) + KT/q \ln N_a N_d/n_{io}^2 \qquad (A.8)$$

At this point, we impose a constraint on the concentration of excess carriers injected into the two sides of the junction. This condition, called law injection, requires that $p_o(x_n) << p(x_n) << n_o(x_n)$ and $no(-x_p) << n(-x_p) << p_o(-x_p)$. Since the excess minority carrier concentration is essentially equal to the excess majority carrier on a point by point basis, low injection implies that the total minority carrier concentration is approximately equal to the excess minority carrier concentration while the total majority carrier concentration can be represented by the equilibrium majority carrier concentration.

Using the low injection approximation on the P side we can write

$$n_o(-x_p) = n_{io}^2/N_a \qquad (A.9)$$

The resulting expression is

$$V_a = KT/q \ln n(-x_p)/n_o(-x_p) \quad (A.10)$$

which can be written

$$n(-x_p) = n_o(-x_p) \exp qV_a/KT \qquad (A.11)$$

In a like manner it can be shown that

$$p(x_n) = p_o(x_n) \exp qV_a/KT \quad (A.12)$$

The preceding equations are the most important boundary conditions for the ideal current-voltage equation.

The hole diffusion equation is now

$$\partial p/\partial t = - p- p_o(x_n)/\tau_p + D_p \partial^2 p/\partial \chi^2 \qquad (A.13)$$

and the Steady-State equation is ($\partial p/\partial t = 0$)

$$d^2p/dx^2 = p\text{-}p_o(x_n)/D_{p\tau p} = p\text{-}p_o(x_n)/L_p{}^2 \quad (A.14)$$

where $L_p = (D_{p\tau p})^{1/2}$ is the diffusion length for holes in the n-type semiconductor. This must now be solved under the conditions $p = p(x_n)$ at $x = x^n$, and $p = p_o(x_n)$ for sufficiently large x. Eqn (A.14) has solutions $\exp[-(x\text{-}x_n)/L_p]$ and $\exp[(x\text{-}x_n)/L_p]$, but the second solution violates the boundary condition for large x; so the full solution of (A.14) is

$$p(x) - p_o(x_n) = [p(x_n)\text{-}p_o(x_n)]\exp(- x\text{-}x_n/L_p)$$

Then,

$$p(x_n) - p_o(x_n) = p_o(x_n)[\exp(qV_a/KT) - 1] \exp(- x\text{-}x_n/L_p) \qquad (A.15)$$

Since the drift term in the hole current density could be neglected, the hole current density $J_p(x_n)$ at x_n is

$$J_p(x_n)= -eD_p\, dp(x)/dx \,|_{x=x_n} = -eD_p\, d/dx \; [p(x)-p_o(x_n)] \,|_{x=x_n} \quad (A.16)$$

Then,

$$J_p(x_n) = qD_p p_o(x_n)/L_p[\exp(qV_a/KT) - 1] \quad (A.17)$$

Similarly,

$$J_n(-x_p) = qD_n n_o(-x_p)/L_n[\exp(qV_a/KT) - 1) \qquad (A.18)$$

where L_n is the diffusion length for the electrons in the p-type semiconductor.

To determine the total current density for the diode we need only find the current density at one point, since the diode is a two-terminal device and we are treating it as a one-dimensional problem. If we assume that the transition region is narrow enough to preclude recombination between $-x_p$ and x_n, the number of electrons per unit time entering the transition region at x_n is equal to the number of electrons per unit time leaving the transition at $-x_p$. This means that the electron current density at those points is the same. Similarly, the hole current density is the same at both edges of the transition region. We can then write

$$J = J_n(x_n) + J_p(x_n) = J_n(-x_p) + J_p(x_n)$$
$$= \{qD_n n_o(-x_p)/L_n + qD_p p_o(x_n)/L_p\} [\exp(qV_a/KT) - 1] \qquad (A.19)$$

If the area of the device is A, I=JA and Eqn.(A.19) can be written as

$$I = I_s[\exp(qV_a/Kt) - 1] \qquad (A.20)$$

where $I_s = J_s A$ and J_s is identified as

$$J_s = qD_n n_o(-x_p)/L_n + qD_p p_o(x_n)/L_p \qquad (A.21)$$

is called the reverse saturation current density. It represents the magnitude of the current density when the applied voltage is large and negative. Eqn.(A.20) is the ideal current-voltage relationship of p-n junction diode.

We next discuss the case when the p and n regions have finite length. The boundary conditions for the holes are

$p(x) = p(x_n)$, at $x=x_n$; $p(x) = p_o(x_n)$, at $x=x_n+W_n$ where $W_n=x_{cn}-x_n$.

Although $\exp[(x-x_n)/L_p]$ and $\exp[-(x-x_n)/L_p]$ are again independent solutions of the diffusion equation, it is more convenient to use as equivalent independent solutions $\sinh[(W_n + x_n - x)/L_p]$ and $\sinh[(x - x_n)/L_p]$. Then

$$p(x) - p_o(x_n) = A\sinh(W_n + x_n - x)/L_p + B\sinh(x-x_n)/L_p \qquad (A.22)$$

Applying the boundary conditions and solving for A and B yields

$$p(x)-p_o(x_n)=[p_o(x_n)\sinh[(x_{cn}-x)/L_p]/\sinh[(x_{cn}-x)/L_p]] \\ [\exp(qV_a)/KT-1] \qquad (A23)$$

Since $J_p(x) = -qD_p\, dp(x)/dx$, using Eq(A.23) we have

$$J_p(x)=[qp_o(x_n)D_p\cosh[(x_{cn}-x)/L_p]/L_p\sinh[x_{cn}-x_n)/L_p]] \\ [\exp(qV_a/KT) - 1] \qquad (A.24)$$

This expression represents the hole current density as a function of position in the region from x_n to x_{cn}. At the boundary of the transition region, the hole current density can be written

$$J_p(x_n)=[qp_o(x_n)D_p/L_p\tanh[(x_{cn}-x_n)/L_p]][\exp(qV_a/KT)-1] \qquad (A.25)$$

Similarly,

$$J_n(-x_p)=[qn_o(-x_p)D_n/L_n\tanh[(x_{cp}-x_p)/L_p]][\exp(qV_a/KT)-1] \qquad (A.26)$$

$$J = J_n(-x_p) + J_p(x_n) \\ =\{qn_o(-x_p)D_n/Ln\tanh[(x_{cp}-x_p)/L_n] + \\ qp_o(x_n)D_p/L_p\tanh[(x_{cn}-x_n)/L_p]\}[\exp(qV_a/KT)-1] \qquad (A27)$$

If we recognize that $n_o(-x_{cp})=n_{io}^2/N_a$ and $p_o(x_n)=n_{io}^2/N_d$ and define $x_{cp}-x_p=W_p$ and $x_{cn}-x_n=W_n$, then

$$J=qn_{io}^2[D_n/N_aL_n\tanh(W_p/L_n) + D_p/N_dL_p\tanh(W_n/L_p)][\exp(qV_a/KT)-1] \quad (A.28)$$

For a device having area A, I=JA and Eq.(A.28) can be written as Eq.(A.20). Here I_s is given as

$$I_s=qn_{io}^2A[D_n/N_aL_n\tan(W_p/L_n) + D_p/N_dL_p\tanh(W_n/Lp)] \quad (A.29)$$

References

1. J.L.Stone, Physics Today, sept. 1993.
2. R.J.Komp, Practical photovoltaics, 2nd ed., 1984.
3. K.W.Boer, International symposium - Workshop on silicon technology development and its role in the sun-belt countries, 14-18 June 1987, Islamabad.
4. D.M.Chapin C.S.Fuller, G.L.Pearson, J.Appl.Phys.25, 1954
5. R.S.Crandall, J.Appl.Phys.53, 3350, 1982.
6. E.Carlson, S.Wagner, 18th IEEE photovoltaic specialists conference, Las Vegas, Nevada, Oct. 21-25, 1985.
7. J.I.Pankove, U.S. Patent No. 4, 109, 271, 1978.
8. Y.Ichikawa, S.Fujikake, S.Saito, H.Ota, T.Yoshida, T.Ihara, H.Sakai, 23rd IEEE photovoltaic specialists conference, Louis, 1993.
9. B.Rech, C.Beneking, Y.G.Michael, T.Eichoff, H.Wagner, Amorphous silicon solar cells technology (to be published).
10. I.Solomon, First international symposium on physics and applications of amorphous semiconductors, Villa Gualino, Torino, 14-18 sept., 1987.
11. T.G.Kim, S.C.Kim, J.M.Jun, K.C.Park, S.Koh, M.K.Han, J.Jang, J.Non-crystalline solids 137 & 138, 1161-1164, 1991, North Holland.
12. T.Yoshida, S.Fujikake, H.Shimabukuro, Y.Ichikawa, H.Sakai, Proc. of 20th IEEE photovoltaic spec. conference, 1988, Las Vegas, Nevada.
13. M.Brodsky, M.Cardona, J.J.Cumo, Phys. Rev. B16, 1977.
14. C.Magee, D.E.Carlson, Solar cells 2, 365, 1980
15. D.E.Carlson, J.Vac.science and technol. 20, 290, 1982a.
16. A.E.Delahoy, R.W.Griffith, Conf. record of 15th IEEE photovoltaic specialists conf., 704, 1981.
17. W.M.Pontuschka, W.E.Carlos, P.C.Tayler, R.W.Griffith, Phys. Rev. B25, 4362, 1982.
18. L.L.Kazmerski, K.A.Emery, Workshop on material sciences and physics of non conventional energy sources (to be published).
19. D.E.Carlson, A.R.Moore, D.J.Szostak, B.Goldestein,

R.W.Smith, P.J.Zanzucchi, W.R.Frenchu, Solar cells 9, 19, 1983b

20. D.L.Staebler, C.R.Wronski, Appl. Phys. Lett. 31, 292, 1977.
21. M.Stutzmann, W.B.Jackson, C.C.Tsai, Phys. Rev. B. 32, 23, 1985.
22. D.Redfield and R.H.Bube, Phys. Rev. Lett. 65, 464,1990.
23. L.Yang, L.Chen, and A.Catalano, Appl. Phys. Lett. 59 (7), 12 August 1991.
24. I.Sakata, Y.Hayashi, IEEE Trans. Electron Devices 32, 551, 1985.
25. D.E.Carlson, Hydrogenated Amorphous Silicon, edited by J.I.Pankove, vol. 21D of semiconductor & semimetals (Academic, Orlando, 1984) P.7.
26. Z.E.Smith, S.Wagner, B.W.Faughan, Appl. Phys. Lett. 46, 1985
27. L.Yang, L.Chen, A.Catalano, Appl. Phys. Lett. 59 (7), 12 August 1991.
28. M.Bennett, J.Newton, K.Rajan, Proc. of 7th European photovoltaic conf., Seville, Spain, P.544, 1986.
29. L.Yang, L.chen, J. Non-crystalline solids 137 & 138, 1991, 1189-1192 North Holland.
30. A.Madan, M.P.Shaw, The physics and applications of amorphous semiconductors, Academic Press, INC., Boston.
31. R.A.Street, Hydrogenated amorphous silicon, Cambridge University Press, Cambridge.
32. N.F.Mott, E.A.Davis, Electronic processes in non-crystalline materials, Oxford University Press, Oxford, 1979.
33. R.C.Chittic, J.H.Alexander, H.F.Sterling, J. Electrocehm. soc. 116, 77, 1969.
34. J.C.Knights, G.Lucovsky, R.J.Nenamich, J. Non-crystalline solids 32, 393,1979.
35. D.E.Carlson, C.R.Wronski, Topics in App. Phys. 36, 291, 1979.
36 W.E.Spear,P.G.LeComber, Solid state communications 17, 1193-1196,1975.

37. W.E.Spear, P.G.LeComber, Pilos. Mag. 43, 407,1976.